

Emergent Anisotropic Non-Fermi Liquid at a Topological Phase Transition in Three Dimensions

SangEun Han,^{1,*} Changhee Lee,^{2,*} Eun-Gook Moon,^{1,†} and Hongki Min^{2,‡}

¹*Department of Physics, Korea Advanced Institute of Science and Technology, Daejeon 305-701, Korea*

²*Department of Physics and Astronomy, Seoul National University, Seoul 08826, Korea*

(Dated: May 14, 2019)

Understanding correlation effects in topological phases and their transitions is a cutting-edge area of research in recent condensed matter physics. We study topological quantum phase transitions (TQPTs) between double-Weyl semimetals (DWSMs) and insulators, and argue that a novel class of quantum criticality appears at the TQPT characterized by emergent *anisotropic* non-Fermi liquid behaviors, in which the interplay between the Coulomb interaction and electronic critical modes induces not only anisotropic renormalization of the Coulomb interaction but also strongly correlated electronic excitation in three spatial dimensions. Using the standard renormalization group methods, large N_f theory and the $\epsilon = 4 - d$ method with fermion flavor number N_f and spatial dimension d , we obtain the anomalous dimensions of electrons ($\eta_f = 0.366/N_f$) in large N_f theory and the associated anisotropic scaling relations of various physical observables. Our results may be observed in candidate materials for DWSMs such as HgCr_2Se_4 or SrSi_2 when the system undergoes a TQPT.

Introduction. — Quantum criticality and topology play key roles in modern condensed matter physics [1–5], and the two concepts become naturally important near TQPTs. Recently, there has been a surge of interest in TQPTs [6–11]. The simplest class is described by the weakly interacting Dirac fermions, and it is well understood that the sign of the Dirac mass terms determines adjacent topological phases [12–14]. Since quasiparticles are well defined, non-interacting tight-binding models are sufficient to describe TQPTs in this class.

Beyond the simplest class, however, our understanding of TQPTs is far from complete. The long-range Coulomb interaction may drastically change the properties of non-interacting fermions near TQPTs, and the non-interacting tight-binding models *cannot* describe some classes of TQPTs. The interplay between critical electronic modes and the Coulomb interaction becomes significant, and quantum critical non-Fermi-liquid states may appear with emergent particle-hole and rotational symmetries [15–19]. Moreover, the interplay may also give rise to weakly coupled but infinitely anisotropic excitations in a class of TQPTs [20–24]. Thus, it is vital to deepen our understanding of TQPTs beyond the simplest class.

In this work, we uncover a novel class of TQPTs which shows emergent *anisotropic* non-Fermi-liquid behaviors in three spatial dimensions (3d) associated with topological nature of electronic wave functions. Our target system is the DWSM adjacent to insulator phases under the long-range Coulomb interaction. The presence of either the fourfold (C_4) or sixfold (C_6) rotational symmetry allows a direct phase transition between DWSMs and insulators whose bare Hamiltonian has a quadratic band

touching spectrum. Without the symmetries, double-Weyl nodes may split into two Weyl nodes. The long-range Coulomb interaction becomes relevant at the critical point, and thus quasi-particle excitations are expected to be absent. Moreover, the absence of the cubic symmetry indicates a possibility of anisotropic quantum critical behaviors in contrast to most of the fixed points with the full rotational symmetry as in conformal field theories. Using the standard renormalization group (RG) methods, we indeed find novel quantum critical phenomena with emergent *anisotropy*. For example, we find that the power-law dependences of the energy dispersion and the Coulomb interaction on momentum become anisotropic, even though they are initially set to be the same in all directions, and all excitations have anomalous dimensions. Our universality class is one concrete example of strongly interacting fixed points with non-Fermi-liquid behaviors beyond the conformal field theory description in 3d. We calculate its experimental signatures in physical observables such as the specific heat, compressibility, diamagnetic susceptibility, and optical conductivity.

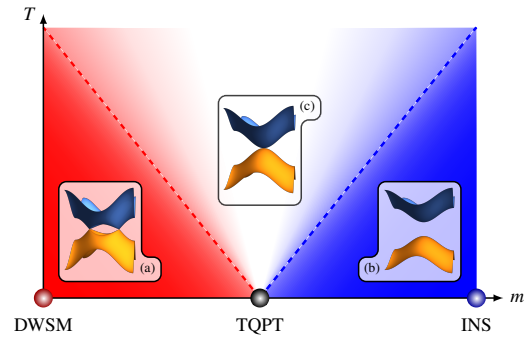


FIG. 1: Phase diagram for the TQPT between the DWSM and insulator phases with the tuning parameter m . The insets show the energy dispersions for the (a) DWSM, (b) insulator and (c) TQPT.

*These authors contributed equally to this work.

†egmoon@kaist.ac.kr

‡hmin@snu.ac.kr

Model. — We consider a minimal lattice model of DWSMs with a C_4 symmetry with a rotational axis along the z direction [25–28, 28, 29],

$$\mathcal{H}(\mathbf{k}) = 2t'_x [\cos(k_y a_0) - \cos(k_x a_0)] \sigma_x + 2t'_y \sin(k_x a_0) \sin(k_y a_0) \sigma_y + 2M_z(\mathbf{k}) \sigma_z, \quad (1)$$

where $M_z(\mathbf{k}) = m_z - t'_z \cos(k_z a_0) + m_0[2 - \cos(k_x a_0) - \cos(k_y a_0)]$ and a_0 is the lattice constant. In general, C_4 symmetry does not imply $t'_x = t'_y$. However, in the presence of the Coulomb interaction, $t'_x = t'_y$ emerges at low energies [29]. For $|m_z| < t'_z$, the Hamiltonian supports two double-Weyl nodes at $\mathbf{k} = (0, 0, \pm k_z^*)$, where $k_z^* = a_0^{-1} \cos^{-1}(m_z/t'_z)$, which are characterized by the Chern numbers ± 2 around the points [25]. For $|m_z| > t'_z$, the system shows an insulator phase. At $|m_z| = t'_z$, a quantum phase transition occurs between the DWSM and insulator phases, as shown in Fig. 1. Neglecting m_0 for simplicity, we obtain the low-energy effective Hamiltonian near the transition point given by

$$\mathcal{H}_0(\mathbf{k}) = t_\perp [(k_x^2 - k_y^2) \sigma_x + 2k_x k_y \sigma_y] + (t_z k_z^2 + m) \sigma_z, \quad (2)$$

where $t_\perp = t'_x a_0^2$ and $t_z = t'_z a_0^2$. Here, a tuning parameter of the TQPT, $m \propto |m_z| - t'_z$, is introduced. The energy eigenvalues of the Hamiltonian are given by $E_\pm(\mathbf{k}) = \pm \sqrt{t_\perp^2 (k_x^2 + k_y^2)^2 + (t_z k_z^2 + m)^2}$, and at $m = 0$ the energy dispersion becomes quadratic in all three directions.

The corresponding effective action with the long-range Coulomb interaction is

$$\mathcal{S} = \int d\tau d^3x \psi^\dagger [\partial_\tau - ig\phi + \mathcal{H}_0(-i\nabla)] \psi + \int d\tau d^3x \frac{1}{2} \left[a \{ (\partial_x \phi)^2 + (\partial_y \phi)^2 \} + \frac{1}{a} (\partial_z \phi)^2 \right], \quad (3)$$

where $g \equiv \frac{\sqrt{4\pi} e_0}{\sqrt{\epsilon}}$ with e_0 and ϵ being the bare charge and the dielectric constant, respectively, ψ is a spinor with $2N_f$ components, and ϕ is a bosonic field describing the long-range Coulomb interaction. Note that the topological aspect of Eq. (2) ensures the band crossing associated with the C_4 symmetry of the system. The parameter a is introduced to characterize the anisotropy ratio of the Coulomb interaction between the xy -plane and the z -axis. For later usage, we define the following dimensionless parameters,

$$\alpha = \frac{A_d - 2g^2}{\sqrt{t_\perp t_z} \Lambda^{4-d}}, \quad \beta = \frac{t_z}{t_\perp}, \quad \gamma = \frac{a\sqrt{\beta}}{2} \quad (4)$$

with $A_d = [6\pi(4\pi)^{\frac{d}{2}} \Gamma(\frac{d}{2})]^{-1}$. Here, α represents the ratio of the Coulomb potential and the electron kinetic energy, β^{-1} is the anisotropy parameter for the fermionic fields, and γ is the combination of the two anisotropy parameters a and β . We assume that all the four-fermion interactions, $u_{ijkl} \psi_i^\dagger \psi_j^\dagger \psi_k \psi_l$, are set to be small at the lattice-spacing scale and flow into the trivial fixed point

as in the literature [30], which is also justified below and in the Supplemental Material [29].

The bare scaling dimensions of the parameters can be obtained by setting $[\tau] = -z$, $[x, y] = -z_\perp$ and $[z] = -1$. We find $[\psi] = (2z_\perp + d - 2)/2$, $[\phi] = (z + z_\perp + d - 3)/2$, and $[g^2] = z - z_\perp - d + 3$. Here, the dimension of the space along the z -axis is extended from the physical dimension of 1 to $d - 2$. This extension is needed for the $\epsilon = 4 - d$ expansion method, as will be explained later. If we set (t_z, t_\perp, a) marginal, $z = 2$ and $z_\perp = 1$ thus, for $d = 3$ the non-interacting fixed point becomes unstable because of the relevant coupling constant g^2 , similar to that of the Luttinger-Abrikosov-Beneslavskii (LAB) phase [17, 31, 32]. We stress that at our fixed point, the system becomes highly *anisotropic* distinguishing the scaling along the z and xy directions, which is fundamentally different from the *isotropic* LAB phase even though the bare scaling gives the same scaling dimensions. In this sense, our fixed point has emergent anisotropy.

To deal with the relevant parameter, we employ the large N_f method and the $\epsilon = 4 - d$ expansion method, and find that both methods give consistent results for the emergent anisotropic non-Fermi-liquid behaviors.

Large N_f calculation. — We first use the large N_f method since it is naturally extended from the conventional random phase approximation [20, 21, 33–35]. The boson self-energy is

$$\Pi(i\Omega, \mathbf{q}) = N_f g^2 \int_{\omega, \mathbf{k}} \text{Tr}[G_0(i\omega + i\Omega, \mathbf{k} + \mathbf{q}) G_0(i\omega, \mathbf{k})], \quad (5)$$

with the fermion propagator $G_0(i\omega, \mathbf{k}) = (-i\omega + \mathcal{H}_0(\mathbf{k}))^{-1}$. Here, we use the notation $\int_{\omega, \mathbf{k}} = \int \frac{d\omega}{2\pi} \frac{dk_x dk_y}{(2\pi)^2} \int' \frac{dk_z}{2\pi}$, where $\int' \frac{dk_z}{2\pi}$ stands for an integration over $\mu < |k_z| < \Lambda$ with the infrared (IR) cutoff μ and the ultra-violet (UV) cutoff Λ . A detailed exposition of the boson self-energy is presented in the Supplemental Material [29]. We propose the following ansatz for the boson self-energy at one-loop level:

$$\Pi(i\Omega, \mathbf{q}) = -\frac{N_f g^2 |q_\perp|}{\sqrt{t_\perp t_z}} F\left(\sqrt{\frac{t_\perp}{|\Omega|}} |q_\perp|, \sqrt{\frac{t_z}{t_\perp}} \left| \frac{q_z}{q_\perp} \right| \right), \quad (6)$$

where $q_\perp \equiv \sqrt{q_x^2 + q_y^2}$ and

$$F(x, y) = \sqrt{C_{\perp 1}^2 + C_{z_1}^2 y^2} \tanh\left(x \sqrt{C_{\perp 2}^2 + C_{z_2}^2 y^2}\right), \quad (7)$$

with $C_{\perp 1} = 0.041$, $C_{\perp 2} = 1.199$, $C_{z_1} = 0.016$, and $C_{z_2} = 1.267$. For the details, see the Supplemental Material [29].

The one-loop boson self-energy modifies the Coulomb potential in momentum space as

$$D(i\Omega, \mathbf{q}) = \frac{1}{D_0^{-1}(\mathbf{q}) - \Pi(i\Omega, \mathbf{q})}, \quad (8)$$

where $D_0(\mathbf{q}) = (aq_\perp^2 + \frac{1}{a} q_z^2)^{-1}$ is the bare boson propagator. In the static ($\Omega = 0$) and long wave length

($q \rightarrow 0$) limit, the self-energy dominates the bare propagator since it linearly depends on the momentum in this limit. Thus, we take the boson self-energy as the main contribution to the renormalized Coulomb interaction, $D(i\Omega, \mathbf{q}) \simeq \frac{1}{-\Pi(i\Omega, \mathbf{q})}$. This indicates that the boson is strongly renormalized from the quadratic to a linear momentum dependence, exhibiting the anomalous dimension of order one at the TQPT. This approximation has been well established in large N_f analysis and is checked afterward.

The fermion self-energy with the renormalized Coulomb interaction is

$$\Sigma(i\omega, \mathbf{k}) = (-ig)^2 \int_{\Omega, \mathbf{q}} G_0(i\omega + i\Omega, \mathbf{k} + \mathbf{q}) D(i\Omega, \mathbf{q}), \quad (9)$$

and the fermion part of the action is modified by the fermion self-energy as

$$-i\omega + \mathcal{H}_0(\mathbf{k}) \rightarrow -i\omega + \mathcal{H}_0(\mathbf{k}) - \Sigma(i\omega, \mathbf{k}). \quad (10)$$

It is straightforward to show that the corrections from the self-energy are logarithmically divergent in both UV and IR cutoffs, respectively, and we find

$$\begin{aligned} \Sigma(i\omega, \mathbf{k}) \approx & \frac{C_\omega}{N_f} (i\omega) \ell - \frac{C_{t_z}}{N_f} \ell (t_z k_z^2) \sigma_z \\ & - \frac{C_{t_\perp}}{N_f} \ell [t_\perp (k_x^2 - k_y^2) \sigma_x + 2t_\perp k_x k_y \sigma_y], \end{aligned} \quad (11)$$

where $C_\omega = 0.366$, $C_{t_\perp} = 0.614$, $C_{t_z} = 0.341$, and $\ell = \log \frac{\Lambda}{\mu}$ is the RG parameter. For the details, see the Supplemental Material [29].

We also evaluate the vertex correction at vanishing external momentum and frequency,

$$\delta_g = (-ig)^2 \int_{\Omega, \mathbf{q}} G_0(i\Omega, \mathbf{q})^2 \frac{1}{-\Pi(i\Omega, \mathbf{q})} = \frac{C_g}{N_f} \ell, \quad (12)$$

where $C_g = 0.366$, which is *exactly* the same as C_ω . This agreement is not a coincidence but instead a consequence of the Ward identity $\delta_g = \partial \Sigma / \partial (i\omega)$.

Using the logarithmic dependence of the self-energy, one can find various anomalous dimensions. The scale invariance at the critical point forces renormalization of the fermion fields with the anomalous dimension $\eta_f = \frac{C_\omega}{N_f}$. The non-zero anomalous dimension clearly indicates non-Fermi-liquid behaviors of the fermionic excitations, which can be understood by the absence of the pole structure in the fermionic Green function.

From Eq. (11), the RG equations for t_\perp and t_z are given by

$$\frac{1}{t_\perp} \frac{dt_\perp}{d\ell} = \frac{C_{t_\perp} - C_\omega}{N_f}, \quad \frac{1}{t_z} \frac{dt_z}{d\ell} = \frac{C_{t_z} - C_\omega}{N_f}. \quad (13)$$

From Eq. (13), we find $\frac{1}{\beta^{-1}} \frac{d\beta^{-1}}{d\ell} = \frac{C_{t_\perp} - C_{t_z}}{N_f} > 0$, indicating that β^{-1} diverges at the TQPT and that the

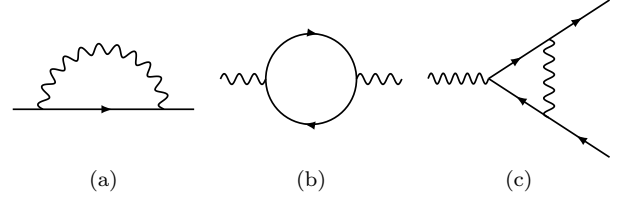


FIG. 2: Feynman diagrams at one-loop order for the (a) fermion self-energy, (b) boson self-energy, and (c) vertex correction. A straight line with an arrowhead and a wavy line represent the fermion and boson propagators, respectively.

fermionic excitations become highly anisotropic at low energies. Thus, our critical theory is described by an emergent anisotropic non-Fermi liquid.

$\epsilon = 4 - d$ expansion. — Our large N_f calculation is further supported by the standard $\epsilon = 4 - d$ expansion [17, 36–38]. Here, we introduce a new renormalization scheme in which the three spatial dimensions are embedded into a manifold that has more coordinates in the direction of the rotational axis (z -direction). Namely, we extend the coordinates as

$$\int \frac{dk_x dk_y}{(2\pi)^2} \int \frac{dk_z}{2\pi} \rightarrow \int \frac{dk_x dk_y}{(2\pi)^2} \int \frac{dk_z d^{d-3}p}{(2\pi)^{d-2}} \quad (14)$$

with $k_z^2 \rightarrow k_z^2 + p^2$, and the momentum \mathbf{p} lives in a $(d-3)$ -dimensional manifold. Recalling $[g^2] = z - z_\perp + 3 - d$ with $z = 2$ and $z_\perp = 1$, the coupling constant becomes marginal at $d = 4$ and the quantum fluctuations give logarithmic divergences. To read off these logarithmic divergences, we introduce the parameter $\epsilon = 4 - d$ and employ the standard momentum shell RG analysis with ϵ expansion. For the momentum shell integration, we impose the UV and IR cutoffs on the $(d-2)$ -dimensional space of (k_z, \mathbf{p}) as

$$\int_{\mathbf{k}, \mathbf{p}} = \int \frac{dk_x dk_y}{(2\pi)^2} \int_{\partial\Lambda} \frac{dk_z d^{d-3}p}{(2\pi)^{d-2}}, \quad (15)$$

where $\partial\Lambda$ represents an infinitesimal momentum shell $\mu < \sqrt{k_z^2 + p^2} < \Lambda$ with $\mu = \Lambda e^{-\ell}$.

By integrating out the high energy modes, we obtain corrections at one-loop order. The fermion self-energy depicted by the diagram in Fig. 2(a) is given by

$$\begin{aligned} \Sigma(i\Omega, \mathbf{q}) = & (-ig)^2 \int_{\omega, \mathbf{k}, \mathbf{p}} G_0(i\omega + i\Omega, \mathbf{k} + \mathbf{q}) D_0(i\omega, \mathbf{k}) \\ \approx & -\alpha F_\perp(\gamma) \ell [t_\perp (q_x^2 - q_y^2) \sigma_x + 2t_\perp q_x q_y \sigma_y] \\ & - \alpha F_z(\gamma) \ell (t_z q_z^2) \sigma_z, \end{aligned} \quad (16)$$

where F_\perp and F_z are dimensionless functions, whose explicit expressions are presented in the Supplemental Material [29]. Note that the frequency part is not renormalized at the one-loop order because of the instantaneous nature of the bare Coulomb interaction. Then, it

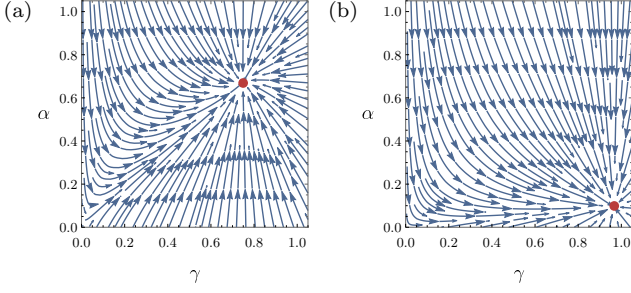


FIG. 3: RG flows of α and γ for (a) $N_f = 1$ and (b) $N_f = 10$ at $\epsilon = 1$. The red dots represent the fixed points (α^*, γ^*) . For $N_f = 1$, $(\alpha^*, \gamma^*) = (0.671, 0.748)$ and for $N_f = 10$, $(\alpha^*, \gamma^*) = (0.096, 0.966)$ obtained from Eq. (18).

is easy to see that the vertex correction [Fig. 2(c)] vanishes due to the Ward identity. For the boson self-energy [Fig. 2(b)], we find

$$\begin{aligned} \Pi(\mathbf{q}) &= N_f g^2 \int_{\omega, \mathbf{k}, \mathbf{p}} \text{Tr} [G_0(i\omega, \mathbf{k} + \mathbf{q}/2) G_0(i\omega, \mathbf{k} - \mathbf{q}/2)] \\ &\approx -N_f \alpha \left[\frac{a}{\gamma} q_{\perp}^2 + \frac{\gamma}{a} q_z^2 \right] \ell. \end{aligned} \quad (17)$$

Renormalizing the wave functions and the coupling constants, we obtain the RG equations for α and γ as

$$\begin{aligned} \frac{1}{\alpha} \frac{d\alpha}{d\ell} &= \epsilon - \frac{N_f \alpha}{2} \left(\frac{1}{\gamma} + \gamma \right) - \frac{\alpha}{2} F_+(\gamma), \\ \frac{1}{\gamma} \frac{d\gamma}{d\ell} &= \frac{N_f \alpha}{2} \left(\frac{1}{\gamma} - \gamma \right) + \frac{\alpha}{2} F_-(\gamma), \end{aligned} \quad (18)$$

where $F_{\pm}(x) = F_z(x) \pm F_{\perp}(x)$. We find two fixed points from the RG equations in Eq. (18). The non-interacting fixed point $\alpha^* = 0$ with arbitrary γ^* is unstable, whereas there exists a stable interacting fixed point at (α^*, γ^*) with $\alpha^* > 0$. For $N_f = 1$ and $\epsilon = 1$, the stable fixed point is located at $(\alpha^*, \gamma^*) = (0.671, 0.748)$, and for large N_f , $(\alpha^*, \gamma^*) \approx (\epsilon/N_f, 1 - 0.358/N_f)$. The RG flows of α and γ are illustrated in Fig. 3.

At the stable fixed point, the RG equations for the bosonic and fermionic anisotropy parameters are given by, respectively,

$$\begin{aligned} \left. \frac{1}{a} \frac{da}{d\ell} \right|_{\text{f.p.}} &= \frac{N_f \alpha^*}{2} \left(\frac{1}{\gamma^*} - \gamma^* \right) > 0, \\ \left. \frac{1}{\beta^{-1}} \frac{d\beta^{-1}}{d\ell} \right|_{\text{f.p.}} &= -\alpha^* F_-(\gamma^*) > 0, \end{aligned} \quad (19)$$

where f.p. stands for the fixed point. Note that β^{-1} diverges at the stable fixed point as in the large N_f calculation demonstrating an emergent anisotropic non-Fermi liquid, which becomes a sanity check of our analysis giving a consistent result with the large N_f calculation. For the details, see the Supplemental Material [29].

Physical observables. — Recently, several materials [26, 39–42] have been proposed as possible candidates

for DWSMs, in which TQPTs may occur by tuning the system parameters. For example, it has been theoretically demonstrated that SrSi₂ can be tuned by changing the lattice constant through doping or strain, leading to a transition from the DWSM to a trivial insulator phase [42]. Since the anisotropic non-Fermi-liquid behavior at the TQPT will provide power-law corrections anisotropically to the scaling of physical observables [34, 43, 44], the anisotropic scaling relations will be valuable to experiments.

First, consider the parameter dependence of physical observables in the non-interacting limit [27–29, 45–48]. The details are presented in the Supplemental Material [29]. In the non-interacting limit, the specific heat C_V , compressibility κ , diamagnetic susceptibility χ_D , and optical conductivity σ are given by

$$\begin{aligned} C_V &\propto \frac{T^{3/2}}{t_{\perp} t_z^{1/2}}, & \kappa &\propto \frac{T^{1/2}}{t_{\perp} t_z^{1/2}}, \\ \chi_{D,\perp} &\propto t_z^{1/2} T^{1/2}, & \chi_{D,z} &\propto \frac{t_{\perp}}{t_z^{1/2}} T^{1/2}, \\ \sigma_{\perp\perp} &\propto \frac{1}{t_z^{1/2}} \Omega^{1/2}, & \sigma_{zz} &\propto \frac{t_z^{1/2}}{t_{\perp}} \Omega^{1/2}. \end{aligned} \quad (20)$$

Here, $\chi_{D,x} = \chi_{D,y} = \chi_{D,\perp}$ and $\sigma_{xx} = \sigma_{yy} = \sigma_{\perp\perp}$ because of the C_4 symmetry of the Hamiltonian. We also assume $t_x = t_y = t_{\perp}$ for simplicity.

Now, consider how the anisotropic non-Fermi liquids change the bare scaling behaviors of the physical observables. From the ϵ expansion, the RG equations for t_{\perp} and t_z are given by

$$\begin{aligned} \frac{1}{t_{\perp}} \frac{dt_{\perp}}{d\ln b} &= z - 2z_{\perp} + \alpha F_{\perp}(\gamma), \\ \frac{1}{t_z} \frac{dt_z}{d\ln b} &= z - 2 + \alpha F_z(\gamma), \end{aligned} \quad (21)$$

where $\ln b \equiv \ell$. Let us choose $z = 2$ and $z_{\perp} = 1$ so that t_{\perp} and t_z are marginal at the tree level. Since $\frac{d\mathcal{O}}{d\ln b} = z\mathcal{O}$ for $\mathcal{O} = \omega, T$ with $z = 2$, $\mathcal{O}(b) = \mathcal{O}b^2$. Let b^* be the cutoff value defined as $\mathcal{O}(b^*) = \Lambda$, then $b^* = (\Lambda/\mathcal{O})^{1/2}$. Combining this with Eq. (21), we find that $t_i(b^*) = t_{i,0}(b^*)^{\alpha^* F_i(\gamma^*)} \propto \mathcal{O}^{-c_i}$ where $i = \perp, z$, $c_i = \frac{1}{2} \left. \frac{d \ln t_i}{d \ln b} \right|_{\text{f.p.}} = \alpha^* F_i(\gamma^*)/2$, $c_{\perp} \approx 0.402/N_f$, and $c_z \approx 0.044/N_f$ in the large N_f approximation.

Then, near the interacting fixed point, the scaling relations of the physical observables with respect to either temperature or frequency become

$$\begin{aligned} C_V &\propto T^{3/2+\eta_1}, & \kappa &\propto T^{1/2+\eta_1}, \\ \chi_{D,\perp} &\propto T^{1/2-\eta_2}, & \chi_{D,z} &\propto T^{1/2-\eta_3}, \\ \sigma_{\perp\perp} &\propto \Omega^{1/2+\eta_2}, & \sigma_{zz} &\propto \Omega^{1/2+\eta_3}, \end{aligned} \quad (22)$$

where $\eta_1 \equiv c_{\perp} + c_z/2 \approx 0.423/N_f$, $\eta_2 \equiv c_z/2 \approx 0.022/N_f$, and $\eta_3 \equiv c_{\perp} - c_z/2 \approx 0.380/N_f$. (Equivalently, we can obtain the same results by including all the effects of

renormalization in the coordinates rather than the system parameters, as presented in the Supplemental Material [29].) Thus, it is easily seen that the diamagnetic susceptibility and optical conductivity show anisotropic scaling behaviors, $\chi_{D,z}/\chi_{D,\perp} \propto T^{\eta_2-\eta_3}$ and $\sigma_{\perp\perp}/\sigma_{zz} \propto \Omega^{\eta_2-\eta_3}$. In addition, the permittivity tensor characterizing the charge screening also exhibits the anisotropic behavior, $\epsilon_{\perp}/\epsilon_z = a^2 \propto \Omega^{\eta_2-\eta_3}$. By measuring these ratios, we can clearly see the anisotropic scaling behaviors at the TQPT.

Discussion and Conclusion. — So far, for simplicity we ignored m_0 in Eq. (1) and the corresponding $s_{\perp}(k_x^2 + k_y^2)\sigma_z$ term with $s_{\perp} = m_0 a_0^2$ in \mathcal{H}_0 , which is allowed by symmetry. If we include the effect of this term, we find that there still exists a stable non-Gaussian fixed point at $(\alpha^*, \gamma^*, \lambda^*) = (0.336\epsilon/N_f, 0.821 - 0.083/N_f, -\text{sgn}(\beta)(0.866 + 0.035/N_f))$ in the ϵ expansion ($\lambda \equiv s_{\perp}/t_{\perp}$), indicating that the anisotropic non-Fermi-liquid behavior is robust against the $s_{\perp}(k_x^2 + k_y^2)\sigma_z$ term. The details are presented in the Supplemental Material [29]. Note that for a TQPT between triple-Weyl semimetals [46], we believe that similar symmetry-allowed parabolic term should be considered.

There are studies on the instability of NFL in the quadratic dispersions under the presence of the short-range interactions [49, 50]. Our calculations are controlled by either ϵ or $1/N_f$. Thus, the scaling dimensions of the four-point short-range interactions at the stable fixed point are the same as the bare one at the leading order, $[u_{ijkl}] = -d + 2 + \mathcal{O}(\epsilon \text{ or } 1/N_f)$, which indicates that our fixed point is stable under the short-range interactions. A detailed discussion on the effect of the short-range interactions can be found in the Supplemental Material [29].

We stress that our emergent anisotropic non-Fermi-liquid fixed point is distinct from previously studied non-Fermi-liquid fixed points. Our fixed point is in 3d in sharp contrast to most of the previously studied fixed points including the very nice work by Sur and Lee where anisotropic non-Fermi liquid below 3d was found [37]. In 3d, quantum fluctuations are typically marginal or even irrelevant, so quasi-particles are usually well-defined. However, the interplay between the topology and C_4 rotational symmetry in our systems protects the quadratic band touching at the topological phase transition, and the anisotropic non-Fermi-liquid fixed point appears. As discussed above, the absence of the cubic symmetry makes the anisotropy even emergent in terms of the anomalous dimensions. Furthermore, the characteristic interplay between topology and symmetry is crucial in addition to the long-range Coulomb interaction to realize our universality class.

In summary, we studied TQPTs between DWsMs and insulators using the large N_f theory and epsilon expansion. We found that a novel class of quantum criticality appears at the TQPT characterized by emergent anisotropic non-Fermi-liquid behaviors in which critical electronic modes and the long-range Coulomb interac-

tion are strongly coupled, and the system becomes infinitely anisotropic. The anisotropic behaviors at the TQPT may be observed experimentally by measuring the power-law corrections to the diamagnetic susceptibility $\chi_{D,z}/\chi_{D,\perp} \propto T^{\eta_2-\eta_3}$ and optical conductivity $\sigma_{\perp\perp}/\sigma_{zz} \propto \Omega^{\eta_2-\eta_3}$, which we propose as smoking-gun signals of our TQPTs.

Acknowledgments

We thank S. X. Zhang, S. K. Jian, and H. Yao for sharing their preprint [51]. C.L. and H.M. were supported by the National Research Foundation of Korea (NRF) grant funded by the Korea government (MSIT) (No. 2018R1A2B6007837) and Creative-Pioneering Researchers Program through Seoul National University (SNU). S.E. Han and E.-G. Moon were supported by the POSCO Science Fellowship of POSCO TJ Park Foundation and NRF of Korea under Grant No. 2017R1C1B2009176.

References

- [1] M. Z. Hasan and C. L. Kane, *Rev. Mod. Phys.* **82**, 3045 (2010).
- [2] X.-L. Qi and S.-C. Zhang, *Rev. Mod. Phys.* **83**, 1057 (2011).
- [3] S. Sachdev and B. Keimer, *Physics Today* **64**, 29 (2011).
- [4] N. P. Armitage, E. J. Mele, and A. Vishwanath, *Rev. Mod. Phys.* **90**, 015001 (2018).
- [5] M. Vojta, *Reports on Progress in Physics* **81**, 064501 (2018).
- [6] B. A. Bernevig, T. L. Hughes, and S.-C. Zhang, *Science* **314**, 1757 (2006).
- [7] M. König, S. Wiedmann, C. Brüne, A. Roth, H. Buhmann, L. W. Molenkamp, X.-L. Qi, and S.-C. Zhang, *Science* **318**, 766 (2007).
- [8] S.-Y. Xu, Y. Xia, L. A. Wray, S. Jia, F. Meier, J. H. Dil, J. Osterwalder, B. Slomski, A. Bansil, H. Lin, R. J. Cava, and M. Z. Hasan, *Science* **332**, 560 (2011).
- [9] Z. Wang, Y. Sun, X.-Q. Chen, C. Franchini, G. Xu, H. Weng, X. Dai, and Z. Fang, *Phys. Rev. B* **85**, 195320 (2012).
- [10] L. Wu, M. Brahlek, R. Valdés Aguilar, A. V. Stier, C. M. Morris, Y. Lubashevsky, L. S. Bilbro, N. Bansal, S. Oh, and N. P. Armitage, *Nature Physics* **9**, 410 (2013).
- [11] Q. Faure, S. Takayoshi, S. Petit, V. Simonet, S. Raymond, L.-P. Regnault, M. Boehm, J. S. White, M. Månsson, C. Rüegg, P. Lejay, B. Canals, T. Lorenz, S. C. Furuya, T. Giamarchi, and B. Grenier, *Nature Physics* **14**, 716 (2018).
- [12] F. D. M. Haldane, *Phys. Rev. Lett.* **61**, 2015 (1988).
- [13] C. L. Kane and E. J. Mele, *Phys. Rev. Lett.* **95**, 226801 (2005).
- [14] L. Fu, C. L. Kane, and E. J. Mele, *Phys. Rev. Lett.* **98**, 106803 (2007).
- [15] J. M. Luttinger, *Phys. Rev.* **102**, 1030 (1956).
- [16] S. Murakami, N. Nagaosa, and S.-C. Zhang, *Phys. Rev. B* **69**, 235206 (2004).

- [17] E.-G. Moon, C. Xu, Y. B. Kim, and L. Balents, *Phys. Rev. Lett.* **111**, 206401 (2013).
- [18] N. Zerf, L. N. Mihaila, P. Marquard, I. F. Herbut, and M. M. Scherer, *Phys. Rev. D* **96**, 096010 (2017).
- [19] M. Hermele, T. Senthil, and M. P. A. Fisher, *Phys. Rev. B* **72**, 104404 (2005).
- [20] Y. Huh and S. Sachdev, *Phys. Rev. B* **78**, 064512 (2008).
- [21] L. Savary, E.-G. Moon, and L. Balents, *Phys. Rev. X* **4**, 041027 (2014).
- [22] B.-J. Yang, E.-G. Moon, H. Isobe, and N. Nagaosa, *Nature Physics* **10**, 774 (2014).
- [23] G. Y. Cho and E.-G. Moon, *Scientific Reports* **6**, 19198 (2016).
- [24] S. Han, G. Y. Cho, and E.-G. Moon, *Phys. Rev. B* **98**, 085149 (2018).
- [25] B. Roy, P. Goswami, and V. Juričić, *Phys. Rev. B* **95**, 201102 (2017).
- [26] C. Fang, M. J. Gilbert, X. Dai, and B. A. Bernevig, *Phys. Rev. Lett.* **108**, 266802 (2012).
- [27] S. Ahn, E. J. Mele, and H. Min, *Phys. Rev. B* **95**, 161112 (2017).
- [28] S.-K. Jian and H. Yao, *Phys. Rev. B* **92**, 045121 (2015).
- [29] See the Supplemental Material for the details of $\epsilon = 4 - d$ expansion method, large N_f calculation, derivations of physical observables in the non-interacting limit, effect of extra perturbations and the sanity check of the power-law corrections for the physical observables, and the effect of the four-point short-range interactions which includes Refs. [17, 40, 43, 48–50].
- [30] D. T. Son, *Phys. Rev. B* **75**, 235423 (2007).
- [31] A. A. Abrikosov and S. D. Beneslavskii, *Soviet Journal of Experimental and Theoretical Physics* **32**, 699 (1971).
- [32] A. A. Abrikosov, *Soviet Journal of Experimental and Theoretical Physics* **39**, 1443 (1974).
- [33] L. Janssen and I. F. Herbut, *Phys. Rev. B* **93**, 165109 (2016).
- [34] H. Isobe, B.-J. Yang, A. Chubukov, J. Schmalian, and N. Nagaosa, *Phys. Rev. Lett.* **116**, 076803 (2016).
- [35] S.-S. Lee, *Phys. Rev. B* **80**, 165102 (2009).
- [36] S. Sachdev, *Quantum Phase Transitions*, 2nd ed. (Cambridge University Press, Cambridge, 2011).
- [37] S. Sur and S.-S. Lee, *Phys. Rev. B* **94**, 195135 (2016).
- [38] S.-S. Lee, *Annual Review of Condensed Matter Physics* **9**, 227 (2018).
- [39] G. Xu, H. Weng, Z. Wang, X. Dai, and Z. Fang, *Phys. Rev. Lett.* **107**, 186806 (2011).
- [40] S.-M. Huang, S.-Y. Xu, I. Belopolski, C.-C. Lee, G. Chang, T.-R. Chang, B. Wang, N. Alidoust, G. Bian, M. Neupane, D. Sanchez, H. Zheng, H.-T. Jeng, A. Bansil, T. Neupert, H. Lin, and M. Z. Hasan, *Proceedings of the National Academy of Sciences* **113**, 1180 (2016).
- [41] Z. Yan and Z. Wang, *Phys. Rev. B* **96**, 041206 (2017).
- [42] B. Singh, G. Chang, T.-R. Chang, S.-M. Huang, C. Su, M.-C. Lin, H. Lin, and A. Bansil, *Scientific Reports* **8**, 10540 (2018).
- [43] D. E. Sheehy and J. Schmalian, *Phys. Rev. Lett.* **99**, 226803 (2007).
- [44] P. Hosur, S. A. Parameswaran, and A. Vishwanath, *Phys. Rev. Lett.* **108**, 046602 (2012).
- [45] J.-R. Wang, W. Li, G. Wang, and C.-J. Zhang, ArXiv e-prints (2018), [arXiv:1802.09050](https://arxiv.org/abs/1802.09050).
- [46] J.-R. Wang, G.-Z. Liu, and C.-J. Zhang, ArXiv e-prints (2018), [arXiv:1802.10365](https://arxiv.org/abs/1802.10365).
- [47] H.-H. Lai, *Phys. Rev. B* **91**, 235131 (2015).
- [48] H. Fukuyama, *Physics Letters A* **32**, 111 (1970).
- [49] I. F. Herbut and L. Janssen, *Phys. Rev. Lett.* **113**, 106401 (2014).
- [50] L. Janssen and I. F. Herbut, *Phys. Rev. B* **92**, 045117 (2015).
- [51] S.-X. Zhang, S.-K. Jian, and H. Yao, arXiv e-prints, [arXiv:1809.10686](https://arxiv.org/abs/1809.10686) (2018), [arXiv:1809.10686](https://arxiv.org/abs/1809.10686) [cond-mat.str-el].

Supplemental Material for “Emergent Anisotropic Non-Fermi Liquid at a Topological Phase Transition in Three Dimensions”

SangEun Han,^{1,*} Changhee Lee,^{2,*} Eun-Gook Moon,^{1,†} and Hongki Min^{2,‡}

¹*Department of Physics, Korea Advanced Institute of Science and Technology, Daejeon 305-701, Korea*

²*Department of Physics and Astronomy, Seoul National University, Seoul 08826, Korea*

I. DETAILS OF THE $\epsilon = 4 - d$ METHOD

In this section, we provide detailed calculations of the $\epsilon = 4 - d$ method. First, we prove that $t_x = t_y$ and $a_x = a_y$ at low energies. Next, we derive the renormalization group (RG) equations using the $\epsilon = 4 - d$ expansion. Then we discuss the effect of the symmetry-allowed parabolic term, which is neglected in the main text, demonstrating that the TQPT is still characterized by anisotropic non-Fermi liquids.

Consider the leading-order self-energy corrections for fermions and bosons:

$$\Sigma(0, \mathbf{k}) = (-ig)^2 \int_{\Omega, \mathbf{q}} G_0(i\Omega, \mathbf{q} + \mathbf{k}) D_0(i\Omega, \mathbf{q}), \quad (\text{S1})$$

$$\Pi(i\Omega, \mathbf{q}) = -N_f (-ig)^2 \int_{\omega, \mathbf{k}} \text{Tr}[G_0(i\Omega + i\omega, \mathbf{k} + \mathbf{q}/2) G_0(i\omega, \mathbf{k} - \mathbf{q}/2)], \quad (\text{S2})$$

where $\int_{\Omega, \mathbf{q}, \mathbf{p}} = \int_{\Omega} \frac{d\Omega}{2\pi} \int \frac{dq_x dq_y}{(2\pi)^2} \int_{\partial\Lambda} \frac{dq_z d^{d-3}p}{(2\pi)^{d-2}}$ with $\partial\Lambda$ being the region $\mu < \sqrt{q_z^2 + p^2} < \Lambda$. Here,

$$G_0(i\Omega, \mathbf{k}) = \frac{1}{-i\Omega + \varepsilon_x(\mathbf{k})\sigma_x + \varepsilon_y(\mathbf{k})\sigma_y + \varepsilon_z(\mathbf{k})\sigma_z} = \frac{i\Omega + \varepsilon_x(\mathbf{k})\sigma_x + \varepsilon_y(\mathbf{k})\sigma_y + \varepsilon_z(\mathbf{k})\sigma_z}{\Omega^2 + E(\mathbf{k})^2}, \quad (\text{S3})$$

$$D_0(i\Omega, \mathbf{q}) = \frac{1}{a_x q_x^2 + a_y q_y^2 + a_z q_z^2}, \quad (\text{S4})$$

where $\varepsilon_x(\mathbf{k}) = t_x(k_x^2 - k_y^2)$, $\varepsilon_y(\mathbf{k}) = 2t_y k_x k_y$, $\varepsilon_z(\mathbf{k}) = t_z k_z^2$, and $E(\mathbf{k}) = \sqrt{\varepsilon_x(\mathbf{k})^2 + \varepsilon_y(\mathbf{k})^2 + \varepsilon_z(\mathbf{k})^2}$.

A. Proof of the emergent rotational symmetry along the k_z -axis

1. Proof of $a_x = a_y$

First, let us prove that $a_x = a_y$ at low energies. From the self-energy of the Coulomb interaction at $\Omega = 0$,

$$\begin{aligned} \Pi(0, \mathbf{k}) &= -N_f (-ig)^2 \int_{\omega, \mathbf{q}} \text{Tr}[G_0(i\omega, \mathbf{q} + \mathbf{k}/2) G_0(i\omega, \mathbf{q} - \mathbf{k}/2)] \\ &= -N_f g^2 \int_{\mathbf{q}, \mathbf{p}} \left(1 - \frac{\vec{\varepsilon}_+ \cdot \vec{\varepsilon}_-}{E_+ E_-}\right) \frac{1}{E_+ + E_-} \\ &\approx -N_f g^2 \int_{\mathbf{q}, \mathbf{p}} \left[\frac{1}{a_x} \frac{(q_x^2 + q_y^2)(t_x^2 t_y^2 (q_x^2 + q_y^2)^2 + t_z^2 (t_x^2 + t_y^2)(q_z^2 + p^2)^2)}{2(t_x^2 (q_x^2 - q_y^2)^2 + 4t_y^2 q_x^2 q_y^2 + t_z^2 (q_z^2 + p^2)^2)^{5/2}} a_x k_x^2 \right. \\ &\quad \left. + \frac{1}{a_y} \frac{(q_x^2 + q_y^2)(t_x^2 t_y^2 (q_x^2 + q_y^2)^2 + t_z^2 (t_x^2 + t_y^2)(q_z^2 + p^2)^2)}{2(t_x^2 (q_x^2 - q_y^2)^2 + 4t_y^2 q_x^2 q_y^2 + t_z^2 (q_z^2 + p^2)^2)^{5/2}} a_y k_y^2 \right] \\ &\quad \left. + \frac{1}{a_z} \frac{t_z^2 q_z^2 (t_x^2 (q_x^2 - q_y^2)^2 + 4t_y^2 q_x^2 q_y^2)}{(t_x^2 (q_x^2 - q_y^2)^2 + 4t_y^2 q_x^2 q_y^2 + t_z^2 (q_z^2 + p^2)^2)^{5/2}} a_z k_z^2 \right], \quad (\text{S5}) \end{aligned}$$

where $\varepsilon_{i\pm} = \varepsilon_i(\mathbf{q} \pm \mathbf{k}/2)$ and $E_{\pm} = \sqrt{\sum_i \varepsilon_{i\pm}^2}$.

We find that the coefficients of the k_x^2 and k_y^2 terms are the same, which we denote as C_a , are given by

$$C_a = -N_f g^2 \int_{\mathbf{q}, \mathbf{p}} \frac{(q_x^2 + q_y^2) [t_x^2 t_y^2 (q_x^2 + q_y^2)^2 + t_z^2 (t_x^2 + t_y^2)(q_z^2 + p^2)^2]}{2 [t_x^2 (q_x^2 - q_y^2)^2 + 4t_y^2 q_x^2 q_y^2 + t_z^2 (q_z^2 + p^2)^2]^{5/2}}$$

$$\propto -\frac{N_f g^2}{\Lambda^{4-d}} \ell, \quad (\text{S6})$$

where $\ell = \ln(\Lambda/\mu)$. Let $C'_a = -C_a/\ell$, which is positive regardless of t_x , t_y and t_z . Then, the beta function of a_x/a_y is

$$\frac{1}{a_x/a_y} \frac{d(a_x/a_y)}{d\ell} = C'_a a_y \left(1 - \frac{a_x}{a_y}\right). \quad (\text{S7})$$

Since C'_a is positive, $a_x = a_y$ at low energies.

2. Proof of $t_x = t_y$

From now on, we employ the following form of the Coulomb interaction propagator with $a_x = a_y \equiv a$ and $a_z = 1/a$,

$$D_0(i\Omega, \mathbf{q}) = \frac{1}{a(q_x^2 + q_y^2) + (q_z^2 + p^2)/a}. \quad (\text{S8})$$

Then

$$\begin{aligned} \Sigma(i\omega, \mathbf{k}) &= (-ig)^2 \int_{\Omega, \mathbf{q}, \mathbf{p}} G_0(i\omega + i\Omega, \mathbf{k} + \mathbf{q}) D_0(i\Omega, \mathbf{q}), \\ &= -\frac{g^2}{2} \int_{\mathbf{q}, \mathbf{p}} \frac{\varepsilon_x(\mathbf{k} + \mathbf{q})\sigma_x + \varepsilon_y(\mathbf{k} + \mathbf{q})\sigma_y + \varepsilon_z(\mathbf{k} + \mathbf{q})\sigma_z}{E(\mathbf{k} + \mathbf{q})} \frac{1}{a(q_x^2 + q_y^2) + (q_z^2 + p^2)/a}, \\ &\approx -\delta_{t_x} \varepsilon_x(\mathbf{k})\sigma_x - \delta_{t_y} \varepsilon_y(\mathbf{k})\sigma_y - \delta_{t_z} \varepsilon_z(\mathbf{k})\sigma_z, \end{aligned} \quad (\text{S9})$$

where

$$\delta_{t_x} = \frac{g^2}{2} \int_{\mathbf{q}, \mathbf{p}} \frac{\varepsilon_x^2 t_y^2 (q_x^4 + 6q_x^2 q_y^2 + q_y^4) - 2\varepsilon_y^2 t_y^2 (q_x^4 + q_y^4) - (2 - t_y^2/t_x^2) \varepsilon_x^2 \varepsilon_z^2 + \varepsilon_z^4}{(\varepsilon_x^2 + \varepsilon_y^2 + \varepsilon_z^2)^{5/2} (a(q_x^2 + q_y^2) + (q_z^2 + p^2)/a)}, \quad (\text{S10})$$

$$\delta_{t_y} = \frac{g^2}{2} \int_{\mathbf{q}, \mathbf{p}} \frac{-\varepsilon_x^2 t_x^2 (q_x^4 + 6q_x^2 q_y^2 + q_y^4) + 2\varepsilon_y^2 t_x^2 (q_x^4 + q_y^4) - (2 - t_x^2/t_y^2) \varepsilon_y^2 \varepsilon_z^2 + \varepsilon_z^4}{(\varepsilon_x^2 + \varepsilon_y^2 + \varepsilon_z^2)^{5/2} (a(q_x^2 + q_y^2) + (q_z^2 + p^2)/a)}, \quad (\text{S11})$$

$$\delta_{t_z} = \frac{g^2}{2} \int_{\mathbf{q}, \mathbf{p}} \frac{(\varepsilon_x^2 + \varepsilon_y^2)(\varepsilon_x^2 + \varepsilon_y^2 - \varepsilon_z t_z (5q_z^2 - p^2))}{(\varepsilon_x^2 + \varepsilon_y^2 + \varepsilon_z^2)^{5/2}} \frac{1}{a(q_x^2 + q_y^2) + (q_z^2 + p^2)/a}. \quad (\text{S12})$$

To prove $t_x = t_y$ at low energies, let us define $T = t_x/t_y$. Then, the beta function of T is given by

$$\frac{1}{T} \frac{dT}{d\ell} = \frac{\delta_{t_x} - \delta_{t_y}}{\ell}. \quad (\text{S13})$$

From Eqs. (S10) and (S11), $\delta_{t_x} - \delta_{t_y}$ is given by

$$\begin{aligned} \delta_{t_x} - \delta_{t_y} &= \frac{g^2}{2} \int_{\mathbf{q}, \mathbf{p}} \frac{(t_x^2 + t_y^2) \varepsilon_x^2 (q_x^4 + 6q_x^2 q_y^2 + q_y^4) - 2(t_x^2 + t_y^2) \varepsilon_y^2 (q_x^4 + q_y^4) - ((2 - t_y^2/t_x^2) \varepsilon_x^2 - (2 - t_x^2/t_y^2) \varepsilon_y^2) \varepsilon_z^2}{(\varepsilon_x^2 + \varepsilon_y^2 + \varepsilon_z^2)^{5/2} (a(q_x^2 + q_y^2) + (q_z^2 + p^2)/a)} \\ &= \frac{g^2}{2t_y} \int_{\mathbf{q}, \mathbf{p}} \frac{(1 + T^2) ((q_x^2 - q_y^2)^2 (q_x^4 + 6q_x^2 q_y^2 + q_y^4) T^2 - 8q_x^2 q_y^2)}{(T^2 (q_x^2 - q_y^2)^2 + 4q_x^2 q_y^2 + \beta^2 (q_z^2 + p^2)^2)^{5/2} (a(q_x^2 + q_y^2) + (q_z^2 + p^2)/a)} \\ &\quad + \frac{g^2}{2t_y} \int_{\mathbf{q}, \mathbf{p}} \frac{\beta^2 (q_z^2 + p^2)^2 (q_x^4 + 6q_x^2 q_y^2 + q_y^4 - 2(q_x^4 + q_y^4) T^2)}{(T^2 (q_x^2 - q_y^2)^2 + 4q_x^2 q_y^2 + \beta^2 (q_z^2 + p^2)^2)^{5/2} (a(q_x^2 + q_y^2) + (q_z^2 + p^2)/a)}, \end{aligned} \quad (\text{S14})$$

where $\beta \equiv t_z/t_y$.

Expanding $\delta_{t_x} - \delta_{t_y}$ in terms of $\delta T = T - 1$, then we have

$$\begin{aligned} \delta_{t_x} - \delta_{t_y} &\approx \frac{g^2}{2t_y} \int_{\mathbf{q}, \mathbf{p}} \frac{(q_x^4 - 6q_x^2 q_y^2 + q_y^4) (2(q_x^2 + q_y^2)^2 - (q_z^2 + p^2)^2 \beta^2)}{((q_x^2 + q_y^2)^2 + \beta^2 (q_z^2 + p^2)^2)^{5/2} (a(q_x^2 + q_y^2) + (q_z^2 + p^2)/a)} \\ &\quad - \frac{g^2}{2t_y} \delta T \int_{\mathbf{q}, \mathbf{p}} \frac{4(q_x^2 + q_y^2)^2 (q_x^8 - 22q_x^6 q_y^2 + 50q_x^4 q_y^4 - 22q_x^2 q_y^6 + q_y^8)}{((q_x^2 + q_y^2)^2 + \beta^2 (q_z^2 + p^2)^2)^{7/2} (a(q_x^2 + q_y^2) + (q_z^2 + p^2)/a)} \end{aligned}$$

$$\begin{aligned}
& + \frac{g^2}{2t_y} \delta T \int_{\mathbf{q}, \mathbf{p}} \frac{\beta^2 (q_z^2 + p^2)^2 (7q_x^8 - 40q_x^6 q_y^2 + 2q_x^4 q_y^4 - 40q_x^2 q_y^6 + 7q_y^8)}{((q_x^2 + q_y^2)^2 + \beta^2 (q_z^2 + p^2)^2)^{7/2} (a(q_x^2 + q_y^2) + (q_z^2 + p^2)/a)} \\
& - \frac{g^2}{2t_y} \delta T \int_{\mathbf{q}, \mathbf{p}} \frac{4\beta^4 (q_x^4 + q_y^4) (q_z^2 + p^2)^4}{((q_x^2 + q_y^2)^2 + \beta^2 (q_z^2 + p^2)^2)^{7/2} (a(q_x^2 + q_y^2) + (q_z^2 + p^2)/a)} \\
& = - \frac{A_{d-2} g^2}{12\pi \sqrt{t_y t_z} \Lambda^{4-d}} \left(\frac{9a^5 \beta^{5/2}}{4} \int_0^\infty dr \frac{r^5 (4a^4 \beta^2 - r^4)}{(r^4 + a^4 \beta^2)^{7/2} (r^2 + 1)} \right) \delta T \ell \\
& = - \alpha G_T(\gamma) \delta T \ell,
\end{aligned} \tag{S15}$$

where $\alpha = \frac{A_{d-2} g^2}{\sqrt{t_\perp t_z} \Lambda^{4-d}}$, $\gamma = \frac{a\sqrt{\beta}}{2}$, and $A_d = \frac{1}{6\pi(4\pi)^{d/2} \Gamma(d/2)}$. Here, we introduce the function $G_T(x)$ defined by

$$\begin{aligned}
G_T(x) & = 72x^5 \int_0^\infty dr \frac{r^5 (64x^4 - r^4)}{(r^4 + 16x^4)^{7/2} (r^2 + 1)} \\
& = \frac{3x}{4(1 + 16x^4)^{7/2}} \left[\sqrt{1 + 16x^4} (1 + 160x^4 - 832x^6 - 1536x^8 + 2048x^{10}) \right. \\
& \quad \left. + 48x^4 (-1 + 64x^4) \ln \left(\frac{4x^2 (4x^2 + \sqrt{1 + 16x^4})}{-1 + \sqrt{1 + 16x^4}} \right) \right].
\end{aligned} \tag{S16}$$

Note that $G_T(\gamma)$ is positive for all γ . Then, we see

$$\frac{1}{\delta T} \frac{d\delta T}{d\ell} \approx - \alpha G_T(\gamma) \delta T \tag{S17}$$

is negative (positive) for positive (negative) δT . Therefore, δT flows to 0, which means $T = 1$ is a stable fixed point and we arrive at the conclusion that $t_x = t_y \equiv t_\perp$ at the low energies. Combining the results of Secs. **IA 1** and **IA 2**, we can use the following form of action at low energies,

$$\mathcal{S} = \int d\tau d^d x \left[\psi^\dagger (\partial_\tau - ig\phi + \hat{\mathcal{H}}_0(-i\nabla)) \psi + \frac{1}{2} \left(a \{ (\partial_x \phi)^2 + (\partial_y \phi)^2 \} + \frac{1}{a} (\partial_z \phi)^2 \right) \right], \tag{S18}$$

where

$$\hat{\mathcal{H}}_0(\mathbf{k}) = t_\perp (k_x^2 - k_y^2) \sigma_x + 2t_\perp k_x k_y \sigma_y + t_z k_z^2 \sigma_z. \tag{S19}$$

B. Renormalization group equations in the $\epsilon = 4 - d$ expansion

In this section, we will show the details of the RG analysis using the $\epsilon = 4 - d$ expansion. From Eqs. (S5) and (S10)–(S12) with $t_x = t_y = t_\perp$ and $a_x = a_y = a_z^{-1} = a$, we obtain the fermion and boson self-energies, respectively, given by

$$\begin{aligned}
\Sigma(i\Omega, \mathbf{q}) & = (-ig)^2 \int_{\omega, \mathbf{k}, \mathbf{p}} G_0(i\omega + i\Omega, \mathbf{k} + \mathbf{q}) D_0(i\omega, \mathbf{k}) \\
& \approx - \alpha F_\perp(\gamma) \ell [t_\perp (q_x^2 - q_y^2) \sigma_x + 2t_\perp q_x q_y \sigma_y] - \alpha F_z(\gamma) \ell (t_z q_z^2) \sigma_z,
\end{aligned} \tag{S20}$$

$$\begin{aligned}
\Pi(\mathbf{q}) & = g^2 \int_{\omega, \mathbf{k}, \mathbf{p}} \text{Tr} [G_0(i\omega, \mathbf{k} + \mathbf{q}/2) G_0(i\omega, \mathbf{k} - \mathbf{q}/2)] \\
& \approx - N_f \alpha \left[\frac{a}{\gamma} q_\perp^2 + \frac{\gamma}{a} q_z^2 \right] \ell,
\end{aligned} \tag{S21}$$

where $F_\perp(\gamma)$ and $F_z(\gamma)$ are given by

$$\begin{aligned}
F_\perp(x) & \equiv \frac{\delta_x}{\alpha \ell} \Big|_{t_x=t_y=t_\perp, a_x=a_y=a_z^{-1}=a} \\
& = 48x^5 \int_0^\infty dr \frac{r(32x^4 - r^4)}{(r^4 + 16x^4)^{5/2} (r^2 + 1)}
\end{aligned}$$

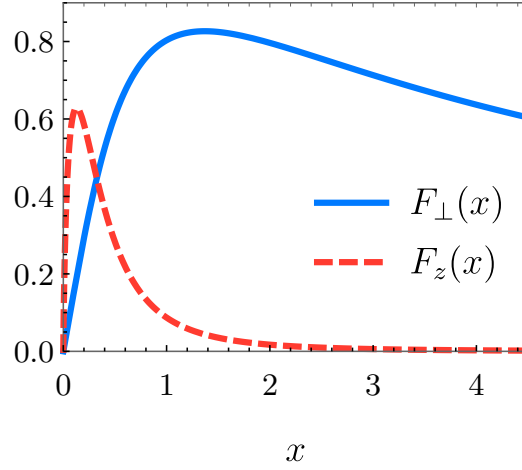


FIG. S1: Plots of $F_{\perp}(x)$ and $F_z(x)$. The blue solid line and red dashed line represent $F_{\perp}(x)$ and $F_z(x)$, respectively.

$$= \frac{3x}{2(1+16x^4)^{5/2}} \left[\sqrt{1+16x^4}(1+64x^4-192x^6) - 16x^4(1-32x^4) \ln \left(\frac{4x^2(4x^2+\sqrt{1+16x^4})}{-1+\sqrt{1+16x^4}} \right) \right], \quad (\text{S22})$$

$$\begin{aligned} F_z(x) &\equiv \frac{\delta_z}{\alpha\ell} \Big|_{t_x=t_y=t_{\perp}, a_x=a_y=a_z^{-1}=a} \\ &= 6x \int_0^{\infty} dr \frac{r^5(r^4-32x^4)}{(r^4+16x^4)^{5/2}(r^2+1)} \\ &= \frac{3x}{(1+16x^4)^{5/2}} \left[\sqrt{1+16x^4}(-2+12x^2+16x^4) + (1-32x^4) \ln \left(\frac{4x^2(4x^2+\sqrt{1+16x^4})}{-1+\sqrt{1+16x^4}} \right) \right]. \end{aligned} \quad (\text{S23})$$

Figure S1 shows the plots of $F_{\perp}(x)$ and $F_z(x)$. Then, after rescaling $z \rightarrow ze^{\ell}$, $(x, y) \rightarrow (x, y)e^{z_{\perp}\ell}$, and $\tau \rightarrow e^{z\ell}\tau$, and introducing the renormalization constant, $\psi \rightarrow \psi/Z_{\psi}^{1/2}$, $\phi \rightarrow \phi/Z_{\phi}^{1/2}$, $t_{\perp} \rightarrow t_{\perp}/Z_{t_{\perp}}$, $t_z \rightarrow t_z/Z_{t_z}$, $a \rightarrow a/Z_a$, and $g \rightarrow g/Z_g$, we arrive at the following renormalized action,

$$\begin{aligned} \mathcal{S}_{\text{renorm}} &= \int d\tau d^d x \left[\psi^{\dagger} \left(\partial_{\tau} - ig\phi + \mathcal{H}_0(-i\nabla) - \Sigma(-i\nabla) \right) \psi + \frac{1}{2} \left(a \{ (\partial_x \phi)^2 + (\partial_y \phi)^2 \} + \frac{1}{a} (\partial_z \phi)^2 \right) - \frac{1}{2} \phi \Pi(-i\nabla) \phi \right] \\ &= \int d\tau d^d x \frac{e^{(z+2z_{\perp}+d-2)\ell}}{Z_{\psi}} \psi^{\dagger} \left[e^{-z\ell} \partial_{\tau} - \frac{1}{Z_g Z_{\phi}^{1/2}} ig\phi \right. \\ &\quad \left. + \frac{e^{-2z_{\perp}\ell}}{Z_{t_{\perp}}} (1 + \alpha F_{\perp}(\gamma)\ell) t_{\perp} ((\partial_y^2 - \partial_x^2)\sigma_x - 2\partial_x \partial_y \sigma_y) - \frac{e^{-2\ell}}{Z_{t_z}} (1 + \alpha F_z(\gamma)) t_z \partial_z^2 \sigma_z \right] \psi \\ &\quad + \int d\tau d^3 x \frac{e^{(z+2z_{\perp}+d-2)\ell}}{2Z_{\phi}} \left[\frac{e^{-2z_{\perp}\ell}}{Z_a} 2 \left(1 + N_f \frac{\alpha}{\gamma} \ell \right) a ((\partial_x \phi)^2 + (\partial_y \phi)^2) + e^{-2\ell} Z_a (1 + N_f \alpha \gamma \ell) \frac{1}{a} (\partial_z \phi)^2 \right]. \end{aligned} \quad (\text{S24})$$

Requiring the scaling invariance of the action, we obtain the renormalization constants as follows:

$$Z_{\psi} = 1 + [2z_{\perp} + (d-2)] \ell, \quad (\text{S25})$$

$$Z_{t_{\perp}} = 1 + [z - 2z_{\perp} + \alpha F_{\perp}(\gamma)] \ell, \quad (\text{S26})$$

$$Z_{t_z} = 1 + [z - 2 + \alpha F_z(\gamma)] \ell, \quad (\text{S27})$$

$$Z_{\phi} = 1 + \left[z + z_{\perp} + (d-3) + \frac{N_f \alpha}{2} \left(\frac{1}{\gamma} + \gamma \right) \right] \ell, \quad (\text{S28})$$

$$Z_a = 1 + \left[1 - z_{\perp} + \frac{N_f \alpha}{2} \left(\frac{1}{\gamma} - \gamma \right) \right] \ell, \quad (\text{S29})$$

$$Z_g = 1 + \left[\frac{z - z_{\perp} - (d-3)}{2} - \frac{N_f \alpha}{4} \left(\frac{1}{\gamma} + \gamma \right) \right] \ell. \quad (\text{S30})$$

From these renormalization constants, we can obtain the following RG equations for $d = 4 - \epsilon$,

$$\frac{1}{t_{\perp}} \frac{dt_{\perp}}{d\ell} = z - 2z_{\perp} + \alpha F_{\perp}(\gamma), \quad (\text{S31})$$

$$\frac{1}{t_z} \frac{dt_z}{d\ell} = z - 2 + \alpha F_z(\gamma), \quad (\text{S32})$$

$$\frac{1}{a} \frac{da}{d\ell} = 1 - z_{\perp} + \frac{N_f \alpha}{2} \left(\frac{1}{\gamma} - \gamma \right), \quad (\text{S33})$$

$$\frac{1}{g^2} \frac{dg^2}{d\ell} = z - z_{\perp} - 1 + \epsilon - \frac{N_f \alpha}{2} \left(\frac{1}{\gamma} + \gamma \right). \quad (\text{S34})$$

Thus, we find the RG equations for the dimensionless parameters α and γ as follows:

$$\frac{1}{\alpha} \frac{d\alpha}{d\ell} = \epsilon - \frac{N_f \alpha}{2} \left(\frac{1}{\gamma} + \gamma \right) - \frac{\alpha}{2} \left(F_z(\gamma) + F_{\perp}(\gamma) \right), \quad (\text{S35})$$

$$\frac{1}{\gamma} \frac{d\gamma}{d\ell} = \frac{N_f \alpha}{2} \left(\frac{1}{\gamma} - \gamma \right) + \frac{\alpha}{2} \left(F_z(\gamma) - F_{\perp}(\gamma) \right). \quad (\text{S36})$$

C. Effects of the symmetry-allowed parabolic term

If we include the symmetry-allowed parabolic term, $s_{\perp}(k_x^2 + k_y^2)\sigma_z$, the non-interacting Hamiltonian \mathcal{H}_0 is modified as

$$\mathcal{H}_0 = t_{\perp}(k_x^2 - k_y^2)\sigma_x + 2t_{\perp}k_x k_y \sigma_y + [Bt_z k_z^2 + s_{\perp}(k_x^2 + k_y^2)]\sigma_z, \quad (\text{S37})$$

where $B = \pm 1$ for the topologically trivial and nontrivial insulator phases, respectively.

1. Boson self-energy

Similarly as in Eq. (S21), we can obtain the boson self-energy in the presence of the symmetry-allowed parabolic term as

$$\begin{aligned} \Pi(i\Omega, \mathbf{q}) &= -N_f (ig)^2 \int_{\omega, \mathbf{k}, \mathbf{p}} \text{Tr}[G_0(i\Omega + i\omega, \mathbf{k} + \mathbf{q})G_0(i\omega, \mathbf{k})] \\ &\approx -N_f \alpha \left[\frac{1}{\gamma} \left(\frac{2 + \lambda^2}{2} - B \frac{\lambda(5 + 2\lambda^2)}{4\sqrt{1 + \lambda^2}} \right) a q_{\perp}^2 + \gamma \left(\frac{1 + 2\lambda^2}{\sqrt{1 + \lambda^2}} - 2B\lambda \right) \frac{1}{a} q_z^2 \right], \end{aligned} \quad (\text{S38})$$

where $\lambda = \frac{s_{\perp}}{t_{\perp}}$.

2. Fermion self-energy

Similarly as in Eq. (S20), we can obtain the fermion self-energy as

$$\begin{aligned} \Sigma(i\omega, \mathbf{k}) &= (ig)^2 \int_{\Omega, \mathbf{q}, \mathbf{p}} G_0(i\omega + i\Omega, \mathbf{k} + \mathbf{q})D_0(i\Omega, \mathbf{q}) \\ &\approx -\delta_{t_{\perp}} [t_{\perp}(k_x^2 - k_y^2)\sigma_x + 2t_{\perp}k_x k_y \sigma_y] - [\delta_{t_z} B t_z k_z^2 + \delta_{s_{\perp}} s_{\perp}(k_x^2 + k_y^2)]\sigma_z, \end{aligned} \quad (\text{S39})$$

where $\delta_{t_{\perp}}$, δ_{t_z} and $\delta_{s_{\perp}}$ are, respectively, given by

$$\begin{aligned} \delta_{t_{\perp}} &= \frac{g^2}{2} \int_{\mathbf{k}, \mathbf{p}} \frac{t_z^2 k_{\perp} k_z^{d+1} (2(Bt_z k_z^2 + s_{\perp} k_{\perp}^2)^2 - t_{\perp}^2 k_{\perp}^4)}{2(t_{\perp}^2 k_{\perp}^4 + (Bt_z k_z^2 + s_{\perp} k_{\perp}^2)^2)^{5/2} (a k_{\perp}^2 + \frac{1}{a} k_z^2)} \\ &= \frac{A_{d-2} g^2 \ell}{\sqrt{t_{\perp} t_z} \Lambda^{4-d}} \int dr \frac{3(2\gamma)^5 r (-r^4 + 2(4B\gamma^2 + \lambda r^2)^2)}{2(1+r^2)(r^4 + (4B\gamma^2 + \lambda r^2)^2)^{5/2}} \end{aligned}$$

$$= \alpha F_{\perp}(\gamma, \lambda) \ell, \quad (\text{S40})$$

$$\begin{aligned} \delta_{t_z} &= \frac{g^2}{2} \int_{\mathbf{k}, \mathbf{p}} \frac{t_{\perp}^3 k_{\perp}^5 k_z^{d-3} (t_{\perp}^2 k_{\perp}^4 - (2Bt_z k_z^2 - s_{\perp} k_{\perp}^2)(Bt_z k_z^2 + s_{\perp} k_{\perp}^2))}{(t_{\perp}^2 k_{\perp}^4 + (Bt_z k_z^2 + s_{\perp} k_{\perp}^2)^2)^{5/2} (ak_{\perp}^2 + \frac{1}{a}k_z^2)} \\ &= \frac{A_{d-2} g^2 \ell}{\sqrt{t_{\perp} t_z} \Lambda^{4-d}} \int dr \frac{6\gamma r^5 (r^4 - (8B\gamma^2 - \lambda r^2)(2B\gamma^2 + \lambda r^2))}{(1+r^2)(r^4 + (4B\gamma^2 + \lambda r^2)^2)^{5/2}} \\ &= \alpha F_z(\gamma, \lambda) \ell, \end{aligned} \quad (\text{S41})$$

$$\begin{aligned} \delta_{s_{\perp}} &= \frac{g^2}{2} \int_{\mathbf{k}, \mathbf{p}} \frac{B t_{\perp}^2 t_z k_{\perp}^3 k_z^{d-1} (t_{\perp}^2 k_{\perp}^4 - (2Bt_z k_z^2 - s_{\perp} k_{\perp}^2)(Bt_z k_z^2 + s_{\perp} k_{\perp}^2))}{s_{\perp} 2(t_{\perp}^2 k_{\perp}^4 + (Bt_z k_z^2 + s_{\perp} k_{\perp}^2)^2)^{5/2} (ak_{\perp}^2 + \frac{1}{a}k_z^2)} \\ &= \frac{B}{\lambda} \frac{A_{d-2} g^2 \ell}{\sqrt{t_{\perp} t_z} \Lambda^{4-d}} \int dr \frac{3(2\gamma)^3 r^3 (r^4 - (8B\gamma^2 - \lambda r^2)(4B\gamma^2 + \lambda r^2))}{(1+r^2)(r^4 + (4B\gamma^2 + \lambda r^2)^2)^{5/2}} \\ &= \frac{B}{\lambda} \alpha F_s(\gamma, \lambda) \ell. \end{aligned} \quad (\text{S42})$$

Here, we introduce the following dimensionless functions,

$$\begin{aligned} F_{\perp}(\gamma, \lambda) &= \int_0^{\infty} dr \frac{48\gamma^5 r (-r^4 + 2(4B\gamma^2 + \lambda r^2)^2)}{(1+r^2)(r^4 + (4B\gamma^2 + \lambda r^2)^2)^{5/2}} \\ &= \frac{3\gamma}{2(1+(4B\gamma^2 - \lambda)^2)} \left[(1+\lambda^2)^{3/2} + 64\gamma^4 (-3\gamma^2 + \sqrt{1+\lambda^2}) - 4B\gamma^2 \lambda (-12\gamma^2 + 5\sqrt{1+\lambda^2}) \right. \\ &\quad \left. - \frac{16\gamma^4 (1 - 2(4B\gamma^2 - \lambda)^2)}{\sqrt{1+(4B\gamma^2 - \lambda)^2}} \ln \left(\frac{4\gamma^2 (4\gamma^2 - B\lambda + \sqrt{1+(4B\gamma^2 - \lambda)^2})}{-1 + 4B\gamma^2 \lambda - \lambda^2 + \sqrt{1+\lambda^2} \sqrt{1+(4B\gamma^2 - \lambda)^2}} \right) \right], \end{aligned} \quad (\text{S43})$$

$$\begin{aligned} F_z(\gamma, \lambda) &= \int_0^{\infty} dr \frac{6\gamma r^5 (r^4 - (8B\gamma^2 - \lambda r^2)(4B\gamma^2 + \lambda r^2))}{(1+r^2)(r^4 + (4B\gamma^2 + \lambda r^2)^2)^{5/2}} \\ &= \frac{3\gamma}{(1+(4B\gamma^2 - \lambda)^2)} \left[-\left(16B\gamma^4 \lambda - 4\gamma^2 (3 + 2\lambda^2) + B\lambda (1 + \lambda^2) \right) + \sqrt{1+\lambda^2} (-2 + (4B\gamma^2 - \lambda)^2) \right. \\ &\quad \left. + \frac{1 - 32\gamma^4 + 4B\gamma^2 \lambda + \lambda^2}{\sqrt{1+(4B\gamma^2 - \lambda)^2}} \ln \left(\frac{4\gamma^2 (4\gamma^2 - B\lambda + \sqrt{1+(4B\gamma^2 - \lambda)^2})}{-1 + 4B\gamma^2 \lambda - \lambda^2 + \sqrt{1+\lambda^2} \sqrt{1+(4B\gamma^2 - \lambda)^2}} \right) \right], \end{aligned} \quad (\text{S44})$$

$$\begin{aligned} F_s(\gamma, \lambda) &= \int_0^{\infty} dr \frac{24\gamma^3 r^3 (r^4 - (8B\gamma^2 - \lambda r^2)(4B\gamma^2 + \lambda r^2))}{(1+r^2)(r^4 + (4B\gamma^2 + \lambda r^2)^2)^{5/2}} \\ &= \frac{-12\gamma}{(1+(4B\gamma^2 - \lambda)^2)} \left[-\left(16B\gamma^4 \lambda - 4\gamma^2 (3 + 2\lambda^2) + B\lambda (1 + \lambda^2) \right) + \sqrt{1+\lambda^2} (-2 + (4B\gamma^2 - \lambda)^2) \right. \\ &\quad \left. - \frac{1 - 32\gamma^4 + 4B\gamma^2 \lambda + \lambda^2}{\sqrt{1+(4B\gamma^2 - \lambda)^2}} \ln \left(\frac{4\gamma^2 (4\gamma^2 - B\lambda + \sqrt{1+(4B\gamma^2 - \lambda)^2})}{-1 + 4B\gamma^2 \lambda - \lambda^2 + \sqrt{1+\lambda^2} \sqrt{1+(4B\gamma^2 - \lambda)^2}} \right) \right] \\ &= -4\gamma^2 F_z(\gamma, \lambda). \end{aligned} \quad (\text{S45})$$

Note that in the limit $\lambda = 0$, $F_{\perp}(\gamma, \lambda) = F_{\perp}(\gamma)$, and $F_z(\gamma, \lambda) = F_z(\gamma)$.

3. RG flow equation

From Sec. IC1 and Sec. IC2, we can obtain the following RG flow equations,

$$\frac{1}{t_{\perp}} \frac{dt_{\perp}}{d\ell} = z - 2z_{\perp} + \alpha F_{\perp}(\gamma, \lambda), \quad (\text{S46})$$

$$\frac{1}{t_z} \frac{dt_z}{d\ell} = z - 2 + \alpha F_z(\gamma, \lambda), \quad (\text{S47})$$

$$\frac{1}{s_{\perp}} \frac{ds_{\perp}}{d\ell} = z - 2z_{\perp} - 4b \frac{\alpha}{\lambda} \gamma^2 F_z(\gamma, \lambda), \quad (\text{S48})$$

$$\frac{1}{a} \frac{da}{d\ell} = 1 - z_{\perp} + \frac{N_f \alpha}{2} \left[\frac{1}{\gamma} \left(\frac{2 + \lambda^2}{2} - B \frac{\lambda(5 + 2\lambda^2)}{4\sqrt{1 + \lambda^2}} \right) - \gamma \left(\frac{1 + 2\lambda^2}{\sqrt{1 + \lambda^2}} - 2B\lambda \right) \right], \quad (\text{S49})$$

$$\frac{1}{g^2} \frac{dg^2}{d\ell} = z - z_{\perp} - 1 + \epsilon - \frac{N_f \alpha}{2} \left[\frac{1}{\gamma} \left(\frac{2 + \lambda^2}{2} - B \frac{\lambda(5 + 2\lambda^2)}{4\sqrt{1 + \lambda^2}} \right) + \gamma \left(\frac{1 + 2\lambda^2}{\sqrt{1 + \lambda^2}} - 2B\lambda \right) \right]. \quad (\text{S50})$$

Then, the RG equations for the dimensionless parameters, α , γ and λ are given by

$$\frac{1}{\alpha} \frac{d\alpha}{d\ell} = \epsilon - \frac{\alpha}{2} \left[N_f \left\{ \frac{1}{\gamma} \left(\frac{2 + \lambda^2}{2} - B \frac{\lambda(5 + 2\lambda^2)}{4\sqrt{1 + \lambda^2}} \right) + \gamma \left(\frac{1 + 2\lambda^2}{\sqrt{1 + \lambda^2}} - 2B\lambda \right) \right\} + F_z(\gamma, \lambda) + F_{\perp}(\gamma, \lambda) \right], \quad (\text{S51})$$

$$\frac{1}{\gamma} \frac{d\gamma}{d\ell} = \frac{\alpha}{2} \left[N_f \left\{ \frac{1}{\gamma} \left(\frac{2 + \lambda^2}{2} - B \frac{\lambda(5 + 2\lambda^2)}{4\sqrt{1 + \lambda^2}} \right) - \gamma \left(\frac{1 + 2\lambda^2}{\sqrt{1 + \lambda^2}} - 2B\lambda \right) \right\} + F_z(\gamma, \lambda) - F_{\perp}(\gamma, \lambda) \right], \quad (\text{S52})$$

$$\frac{1}{\lambda} \frac{d\lambda}{d\ell} = -\frac{\alpha}{\lambda} [4B\gamma^2 F_z(\gamma, \lambda) + \lambda F_{\perp}(\gamma, \lambda)]. \quad (\text{S53})$$

For given N_f , the RG equations have unstable fixed point, $\alpha^* = 0$ with arbitrary γ^* and λ^* , and stable interacting fixed point, $(\alpha^*, \gamma^*, \lambda^*) = (0.342\epsilon/N_f, 0.799 - 0.079/N_f, -B(0.875 + 0.032/N_f))$ for large N_f . Then, near the interacting fixed point,

$$\left. \frac{1}{a} \frac{da}{d\ell} \right|_{\text{f.p.}} = \frac{N_f \alpha^*}{2} \left[\frac{1}{\gamma^*} \left(\frac{2 + \lambda^{*2}}{2} - B \frac{\lambda^*(5 + 2\lambda^{*2})}{4\sqrt{1 + \lambda^{*2}}} \right) - \gamma^* \left(\frac{1 + 2\lambda^{*2}}{\sqrt{1 + \lambda^{*2}}} - 2B\lambda^* \right) \right] > 0, \quad (\text{S54})$$

$$\left. \frac{1}{\beta^{-1}} \frac{d\beta^{-1}}{d\ell} \right|_{\text{f.p.}} = -\alpha^* (F_z(\gamma^*, \lambda^*) - F_{\perp}(\gamma^*, \lambda^*)) > 0. \quad (\text{S55})$$

Thus, the bosonic and fermionic anisotropy parameters a and β^{-1} diverge at the stable interacting fixed point. Therefore, even if we keep $s_{\perp}(k_x^2 + k_y^2)\sigma_z$, the interacting fixed point still exhibits anisotropic non-Fermi liquid behaviors.

II. DETAILS OF THE LARGE N_f CALCULATION

In this section, we will show the detailed calculations of the large N_f method.

A. Boson self-energy

Consider the self-energy of the Coulomb interaction given by

$$\begin{aligned} \Pi(i\Omega, \mathbf{q}) &= -N_f (-ig)^2 \int_{\omega, \mathbf{k}} \text{Tr}[G_0(i\Omega + i\omega, \mathbf{k} + \mathbf{q})G_0(i\omega, \mathbf{k})] \\ &= -N_f g^2 \int_{\mathbf{k}} \frac{E_+ + E_-}{(E_+ + E_-)^2 + \Omega^2} \left(1 - \frac{\vec{\epsilon}_+ \cdot \vec{\epsilon}_-}{E_+ E_-} \right), \end{aligned} \quad (\text{S56})$$

where $\varepsilon_{i\pm} = \varepsilon_i(\mathbf{k} \pm \mathbf{q}/2)$ and $E_{\pm} = \sqrt{\sum_i \varepsilon_{i\pm}^2}$.

1. q_{\perp} dependence

Let us find the q_{\perp} dependence in $\Pi(i\Omega, \mathbf{q})$ with non-zero $i\Omega$. Because of the emergent rotational symmetry along the k_z -axis, we put $\mathbf{q}_{\perp} = q_{\perp} \hat{x}$ for simplicity. After changing the integration variables, $k_x \rightarrow q_{\perp} x$, $k_y \rightarrow q_{\perp} y$, $k_z \rightarrow (t_{\perp}/t_z)^{1/2} q_{\perp} z$, we get

$$\Pi(i\Omega, q_{\perp}) = -\frac{N_f g^2 |q_{\perp}|}{8\pi^3 \sqrt{t_{\perp} t_z}} \int d^3x \frac{\sqrt{\left((x+1)^2 + y^2 \right)^2 + z^4} + \sqrt{\left(x^2 + y^2 \right)^2 + z^4}}{\left[\sqrt{\left((x+1)^2 + y^2 \right)^2 + z^4} + \sqrt{\left(x^2 + y^2 \right)^2 + z^4} \right]^2 + \left(\frac{\Omega}{t_{\perp} |q_{\perp}|} \right)^2}$$

$$\begin{aligned}
& \times \left[1 - \frac{\left((x+1)^2 - y^2 \right) \left(x^2 - y^2 \right) + 4(x+1)xy^2 + z^4}{\sqrt{\left((x+1)^2 + y^2 \right)^2 + z^4} \sqrt{\left(x^2 + y^2 \right)^2 + z^4}} \right] \\
& = -\frac{C_{\perp 1} N_f g^2}{\sqrt{t_{\perp}^2 t_z}} \sqrt{t_{\perp} q_{\perp}^2} \tanh(C_{\perp 2} \xi_r),
\end{aligned} \tag{S57}$$

where $\xi_r = \sqrt{\frac{t_{\perp}}{|\Omega|}} |q_{\perp}|$, $C_{\perp 1} = 0.042$, and $C_{\perp 2} = 1.199$. The final result is a fitting function using an ansatz obtained from $\Pi(i\Omega, q_{\perp}) \propto \xi_r^2$ for $\xi_r \ll 1$, and $\Pi(i\Omega, q_{\perp}) \propto \xi_r$ for $\xi_r \gg 1$.

2. q_z dependence

Similarly, after changing the integration variables, $k_{\perp} \rightarrow (t_z/t_{\perp})^{1/2} q_{\perp} r$, $k_z \rightarrow q_z z$, we get

$$\begin{aligned}
\Pi(i\Omega, q_z) &= -\frac{N_f g^2 |q_z|}{4\pi^2 t_{\perp}} \int_0^{\infty} dr r \int_{-\infty}^{\infty} dz \frac{\sqrt{r^4 + (z+1)^4} + \sqrt{r^4 + z^4}}{\left[\sqrt{r^4 + (z+1)^4} + \sqrt{r^4 + z^4} \right]^2 + \left(\frac{\Omega}{t_z q_z} \right)^2} \\
& \times \left[1 - \frac{r^4 + (z+1)^2 z^2}{\sqrt{r^4 + (z+1)^4} \sqrt{r^4 + z^4}} \right] \\
& = -\frac{C_{z1} N_f g^2}{\sqrt{t_{\perp}^2 t_z}} \sqrt{t_z q_z^2} \tanh(C_{z2} \xi_z),
\end{aligned} \tag{S58}$$

where $\xi_z = \sqrt{\frac{t_z}{|\Omega|}} |q_z|$, $C_{z1} = 0.016$, and $C_{z2} = 1.267$. The final result is a fitting function using an ansatz obtained from $\Pi(i\Omega, q_z) \propto \xi_z^2$ for $\xi_z \ll 1$, and $\Pi(i\Omega, q_z) \propto \xi_z$ for $\xi_z \gg 1$.

3. Arbitrary q dependence

For arbitrary \mathbf{q} ,

$$\begin{aligned}
\Pi(i\Omega, \mathbf{q}) &= -\frac{N_f g^2 |q_{\perp}|}{8\pi^3 \sqrt{t_{\perp} t_z}} \frac{\xi_z}{\xi_r} \int d^3 x \frac{\sqrt{\left((x+1)^2 + y^2 \right)^2 + \frac{\xi_z^4}{\xi_r^4} (z+1)^4} + \sqrt{\left(x^2 + y^2 \right)^2 + \frac{\xi_z^4}{\xi_r^4} z^4}}{\left[\sqrt{\left((x+1)^2 + y^2 \right)^2 + \frac{\xi_z^4}{\xi_r^4} (z+1)^4} + \sqrt{\left(x^2 + y^2 \right)^2 + \frac{\xi_z^4}{\xi_r^4} z^4} \right]^2 + \left(\frac{\Omega}{t_{\perp} q_{\perp}} \right)^2} \\
& \times \left[1 - \frac{\left((x+1)^2 - y^2 \right) \left(x^2 - y^2 \right) + 4(x+1)xy^2 - \frac{\xi_z^4}{\xi_r^4} (z+1)z}{\sqrt{\left((x+1)^2 + y^2 \right)^2 + \frac{\xi_z^4}{\xi_r^4} (z+1)^4} \sqrt{\left(x^2 + y^2 \right)^2 + \frac{\xi_z^4}{\xi_r^4} z^4}} \right] \\
& = -\frac{N_f g^2}{\sqrt{t_{\perp}^2 t_z}} \sqrt{C_{\perp 1}^2 t_{\perp} q_{\perp}^2 + C_{z1}^2 t_z q_z^2} \tanh \left(\sqrt{C_{\perp 2}^2 \xi_r^2 + C_{z2}^2 \xi_z^2} \right).
\end{aligned} \tag{S59}$$

For $\Pi(i\Omega, \mathbf{q}) \equiv -\frac{N_f g^2 |q_{\perp}|}{\sqrt{t_{\perp} t_z}} F \left(\sqrt{\frac{t_{\perp}}{|\Omega|}} |q_{\perp}|, \sqrt{\frac{t_z}{t_{\perp}}} \left| \frac{q_z}{q_{\perp}} \right| \right)$, we illustrate the dimensionless function $F(x, y)$ in Fig. S2(a) and compare it with the exact numerical values in Fig. S2(b).

B. Fermion self-energy

Using the boson self-energy obtained in Sec. II A, we can obtain the fermion self-energy as follows:

$$\Sigma(i\omega, \mathbf{k}) = (ig)^2 \int_{\Omega, \mathbf{q}} G_0(i\Omega + i\omega, \mathbf{q} + \mathbf{k}) D(i\Omega, \mathbf{q})$$

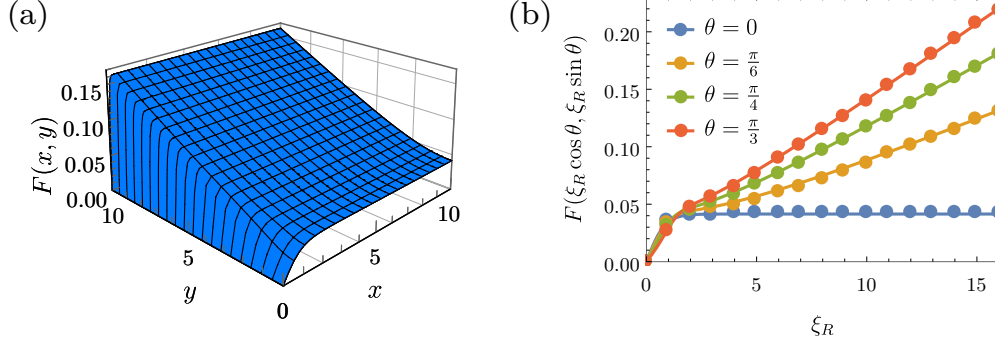


FIG. S2: (a) The dimensionless function $F(x, y)$. (b) Comparison between the exact numerical values and the ansatz $F(x, y)$. For $\sqrt{\frac{t_\perp}{|\Omega|}}|q_\perp| = \xi_R \cos \theta$ and $\sqrt{\frac{t_z}{t_\perp}}\left|\frac{q_z}{q_\perp}\right| = \xi_R \sin \theta$, we present the numerical and analytic values for $\theta = 0$ (blue), $\pi/6$ (yellow), $\pi/4$ (green), and $\pi/3$ (red). The dotted points represent the exact numerical values, and the solid lines represent the values obtained by the ansatz in Eq. (6). The ansatz is in good agreement with the exact numerical values.

$$\begin{aligned}
&= -g^2 \int_{\Omega, \mathbf{q}} \frac{i(\Omega + \omega) + \varepsilon_x(\mathbf{k} + \mathbf{q})\sigma_x + \varepsilon_y(\mathbf{k} + \mathbf{q})\sigma_y + \varepsilon_z(\mathbf{k} + \mathbf{q})\sigma_z}{(\Omega + \omega)^2 + \varepsilon_x^2(\mathbf{k} + \mathbf{q}) + \varepsilon_y^2(\mathbf{k} + \mathbf{q}) + \varepsilon_z^2(\mathbf{k} + \mathbf{q})} \frac{1}{a(q_x^2 + q_y^2) + q_z^2/a - \Pi(i\Omega, \mathbf{q})} \\
&\approx -g^2 \int_{\Omega, \mathbf{q}} \frac{i(\Omega + \omega) + \varepsilon_x(\mathbf{k} + \mathbf{q})\sigma_x + \varepsilon_y(\mathbf{k} + \mathbf{q})\sigma_y + \varepsilon_z(\mathbf{k} + \mathbf{q})\sigma_z}{(\Omega + \omega)^2 + \varepsilon_x^2(\mathbf{k} + \mathbf{q}) + \varepsilon_y^2(\mathbf{k} + \mathbf{q}) + \varepsilon_z^2(\mathbf{k} + \mathbf{q})} \frac{1}{-\Pi(i\Omega, \mathbf{q})} \\
&\approx i\omega\delta_\omega - \delta_{t_\perp}(\varepsilon_x(\mathbf{k})\sigma_x + \varepsilon_y(\mathbf{k})\sigma_y) - \delta_{t_z}\varepsilon_z(\mathbf{k})\sigma_z.
\end{aligned} \tag{S60}$$

The corrections δ_ω , δ_{t_\perp} , and δ_{t_z} are evaluated in the following subsections.

1. ω correction δ_ω

The correction δ_ω is given by

$$\begin{aligned}
\delta_\omega &= -g^2 \int_{\Omega, \mathbf{q}} \frac{t_\perp^2(q_x^2 + q_y^2)^2 + t_z^2 q_z^4 - \Omega^2}{[t_\perp^2(q_x^2 + q_y^2)^2 + t_z^2 q_z^4 + \Omega^2]^2} \frac{\coth\left(\frac{\sqrt{C_{\perp 2}^2(q_x^2 + q_y^2) + C_{z 2}^2 \beta q_z^2}}{(\Omega/t_\perp)^{1/2}}\right)}{\frac{N_f e^2}{(t_\perp t_z)^{1/2}} \sqrt{C_{\perp 1}^2(q_x^2 + q_y^2) + C_{z 1}^2 \beta q_z^2}} \\
&= -\frac{(t_\perp t_z)^{1/2}}{8\pi^3 N_f} \frac{1}{t_\perp^2} \int_{-\infty}^{\infty} d\Omega \int_{\mu < |q_z| < \Lambda} dq_z \int_{-\infty}^{\infty} dq_\perp q_\perp \frac{q_\perp^4 + \beta^2 q_z^4 - \Omega^2/t_\perp^2}{[q_\perp^4 + \beta^2 q_z^4 + \Omega^2/t_\perp^2]^2} \frac{\coth\left(\frac{\sqrt{C_{\perp 2}^2 q_\perp^2 + C_{z 2}^2 \beta q_z^2}}{(\Omega/t_\perp)^{1/2}}\right)}{\sqrt{C_{\perp 1}^2 q_\perp^2 + C_{z 1}^2 \beta q_z^2}}.
\end{aligned} \tag{S61}$$

After changing the integration variables, $q_\perp \rightarrow \sqrt{\beta} q_z a$ and $\Omega \rightarrow \beta t_\perp q_z^2 b$, we have

$$\begin{aligned}
\delta_\omega &= \frac{(t_\perp t_z)^{1/2}}{N_f} \frac{1}{t_\perp^2} \frac{t_\perp \beta^2}{\beta^{5/2}} \ln(\Lambda/\mu) \int_0^\infty da \int_0^\infty db \frac{a}{2\pi^3} \frac{-a^2 - 1 + b^2}{(a^4 + 1 + b^2)^2} \frac{\coth\left(\frac{\sqrt{(C_{\perp 2}^2 a^2 + C_{z 2}^2)}/b}}{\sqrt{C_{\perp 1}^2 a^2 + C_{z 1}^2}}\right)}{\sqrt{C_{\perp 1}^2 a^2 + C_{z 1}^2}} \\
&= \frac{C_\omega}{N_f} \ln(\Lambda/\mu),
\end{aligned} \tag{S62}$$

where $C_\omega = 0.366072$. Note that δ_ω has a logarithmic divergence both in the UV and IR cutoffs.

2. t_\perp correction δ_{t_\perp}

The correction δ_{t_\perp} is given by

$$\begin{aligned} \delta_{t_\perp} &= g^2 \int_{\Omega, \mathbf{q}} \frac{(\Omega^2 + t_z^2 q_z^4)(\Omega^2 - 3t_\perp^2 (q_x^2 + q_y^2)^2 + t_z^2 q_z^4)}{[\Omega^2 + t_\perp^2 (q_x^2 + q_y^2)^2 + t_z^2 q_z^4]^3} \frac{\coth\left(\frac{\sqrt{C_{\perp 2}^2 (q_x^2 + q_y^2) + C_{z 2}^2 \beta q_z^2}}{(\Omega/t_\perp)^{1/2}}\right)}{\frac{N_f e^2}{(t_\perp t_z)^{1/2}} \sqrt{C_{\perp 1}^2 (q_x^2 + q_y^2) + C_{z 1}^2 \beta q_z^2}} \\ &= \frac{(t_\perp t_z)^{1/2}}{8\pi^3 t_\perp^2 N_f} \int_{-\infty}^{\infty} d\Omega \int_{\mu < |q_z| < \Lambda} dq_z \int_{-\infty}^{\infty} dq_\perp q_\perp \frac{(\Omega^2/t_\perp^2 + \beta^2 q_z^4)(\Omega^2/t_\perp^2 - 3q_\perp^4 + \beta^2 q_z^4)}{[\Omega^2/t_\perp^2 + q_\perp^4 + \beta^2 q_z^4]^3} \frac{\coth\left(\frac{\sqrt{C_{\perp 2}^2 q_\perp^2 + C_{z 2}^2 \beta q_z^2}}{(\Omega/t_\perp)^{1/2}}\right)}{\sqrt{C_{\perp 1}^2 q_\perp^2 + C_{z 1}^2 \beta q_z^2}}. \end{aligned} \quad (\text{S63})$$

After changing the integration variables, $q_\perp \rightarrow \sqrt{\beta} q_z a$ and $\Omega \rightarrow \beta t_\perp q_z^2 b$, we have

$$\begin{aligned} \delta_{t_\perp} &= \frac{(t_\perp t_z)^{1/2}}{t_\perp^2 N_f} \frac{t_\perp \beta^2}{\beta^{5/2}} \ln(\Lambda/\mu) \int_0^\infty da \int_0^\infty db \frac{a}{2\pi^3} \frac{(1+b^2)(-3a^4 + 1 + b^2)}{(a^4 + 1 + b^2)^3} \frac{\coth\left(\frac{\sqrt{(C_{\perp 2}^2 a^2 + C_{z 2}^2)/b}}{\sqrt{C_{\perp 1}^2 a^2 + C_{z 1}^2}}\right)}{\sqrt{C_{\perp 1}^2 a^2 + C_{z 1}^2}} \\ &= \frac{C_{t_\perp}}{N_f} \ln(\Lambda/\mu), \end{aligned} \quad (\text{S64})$$

where $C_{t_\perp} = 0.614362$. Note that δ_{t_\perp} has a logarithmic divergence both in the UV and IR cutoffs.

3. t_z correction δ_{t_z}

The correction δ_{t_z} is given by

$$\begin{aligned} \delta_{t_z} &= g^2 \int_{\Omega, \mathbf{q}} \frac{16t_z^4 q_z^8 + \left(\Omega^2 + t_\perp^2 (q_x^2 + q_y^2)^2 + t_z^2 k_z^4\right) \left(\Omega^2 + t_\perp^2 (q_x^2 + q_y^2)^2 - 13t_z^2 k_z^4\right)}{[\Omega^2 + t_\perp^2 (q_x^2 + q_y^2)^2 + t_z^2 q_z^4]^3} \\ &\quad \times \frac{\coth\left(\frac{\sqrt{C_{\perp 2}^2 (q_x^2 + q_y^2) + C_{z 2}^2 \beta q_z^2}}{(\Omega/t_\perp)^{1/2}}\right)}{\frac{N_f e^2}{(t_\perp t_z)^{1/2}} \sqrt{C_{\perp 1}^2 (q_x^2 + q_y^2) + C_{z 1}^2 \beta q_z^2}} \end{aligned} \quad (\text{S65})$$

$$\begin{aligned} &= \frac{(t_\perp t_z)^{1/2}}{8\pi^3 t_\perp^2 N_f} \int_{-\infty}^{\infty} d\Omega \int_{\mu < |q_z| < \Lambda} dq_z \int_{-\infty}^{\infty} dq_\perp q_\perp \frac{16\beta^4 q_z^8 + \left(\Omega^2/t_\perp^2 + q_\perp^4 + \beta^2 k_z^4\right) \left(\Omega^2/t_\perp^2 + q_\perp^4 - 13\beta^2 k_z^4\right)}{[\Omega^2/t_\perp^2 + q_\perp^4 + \beta^2 q_z^4]^3} \\ &\quad \times \frac{\coth\left(\frac{\sqrt{C_{\perp 2}^2 q_\perp^2 + C_{z 2}^2 \beta q_z^2}}{(\Omega/t_\perp)^{1/2}}\right)}{\sqrt{C_{\perp 1}^2 q_\perp^2 + C_{z 1}^2 \beta q_z^2}}. \end{aligned} \quad (\text{S66})$$

After changing the integration variables, $q_\perp \rightarrow \sqrt{\beta} q_z a$ and $\Omega \rightarrow \beta t_\perp q_z^2 b$, we have

$$\begin{aligned} \delta_{t_z} &= \frac{(t_\perp t_z)^{1/2}}{t_\perp^2 N_f} \frac{t_\perp \beta^2}{\beta^{5/2}} \ln(\Lambda/\mu) \int_0^\infty da \int_0^\infty db \frac{a}{2\pi^3} \frac{16 + (a^4 + 1 + b^2)(a^4 - 13 + b^2)}{(a^4 + 1 + b^2)^3} \frac{\coth\left(\frac{\sqrt{(C_{\perp 2}^2 a^2 + C_{z 2}^2)/b}}{\sqrt{C_{\perp 1}^2 a^2 + C_{z 1}^2}}\right)}{\sqrt{C_{\perp 1}^2 a^2 + C_{z 1}^2}} \\ &= \frac{C_{t_z}}{N_f} \ln(\Lambda/\mu), \end{aligned} \quad (\text{S67})$$

where $C_{t_z} = 0.341231$. Note that δ_{t_z} has a logarithmic divergence both in the UV and IR cutoffs.

C. Vertex correction

The correction δ_g is given by

$$\begin{aligned}
\delta_g &= (ig)^2 \int_{\Omega, \mathbf{q}} \frac{1}{2} \text{Tr}[G_0(i\omega, \mathbf{q})G_0(i\omega, \mathbf{q})]D(i\omega, \mathbf{q}) \\
&= -g^2 \int_{\Omega, \mathbf{q}} \frac{-\Omega^2 + t_\perp^2 (q_x^2 + q_y^2)^2 + t_z^2 q_z^4}{[\Omega^2 + t_\perp^2 (q_x^2 + q_y^2)^2 + t_z^2 q_z^4]^2} \frac{\coth\left(\sqrt{(C_{\perp 2}^2 (q_x^2 + q_y^2) + C_{z 2}^2 \beta q_z^2)} t_\perp / \Omega\right)}{\frac{N_f e^2}{\sqrt{t_\perp t_z}} \sqrt{C_{\perp 1}^2 (q_x^2 + q_y^2) + C_{z 1}^2 \beta q_z^2}} \\
&= -\frac{\sqrt{t_\perp t_z}}{8\pi^3 N_f t_\perp^2} \int_{-\infty}^{\infty} d\Omega \int_{\mu < |q_z| < \Lambda} dq_z \int_{-\infty}^{\infty} dq_\perp q_\perp \frac{-\Omega^2/t_\perp^2 + q_\perp^4 + \beta^2 q_z^4}{(\Omega^2/t_\perp^2 + q_\perp^4 + \beta^2 q_z^4)^2} \frac{\coth\left(\sqrt{(C_{\perp 2}^2 q_\perp^2 + C_{z 2}^2 \beta q_z^2)} t_\perp / \Omega\right)}{\sqrt{C_{\perp 1}^2 q_\perp^2 + C_{z 1}^2 \beta q_z^2}}. \quad (\text{S68})
\end{aligned}$$

After changing the integration variables, $q_\perp \rightarrow \sqrt{\beta} q_z a$ and $\Omega \rightarrow \beta t_\perp q_z^2 b$, we have

$$\begin{aligned}
\delta_g &= \frac{(t_\perp t_z)^{1/2}}{N_f} \frac{1}{t_\perp^2} \frac{t_\perp \beta^2}{\beta^{5/2}} \ln(\Lambda/\mu) \int_0^\infty da \int_0^\infty db \frac{a}{2\pi^3} \frac{-a^2 - 1 + b^2}{(a^4 + 1 + b^2)^2} \frac{\coth\left(\sqrt{(C_{\perp 2}^2 a^2 + C_{z 2}^2)} b\right)}{\sqrt{C_{\perp 1}^2 a^2 + C_{z 1}^2}} \\
&= \frac{C_g}{N_f} \ln(\Lambda/\mu), \quad (\text{S69})
\end{aligned}$$

where $C_g = C_\omega$, which is consistent with the Ward identity.

III. CONSISTENCY BETWEEN THE LARGE N_f CALCULATION AND ϵ EXPANSION

In this section, we will show the correspondence between the large N_f calculation and the ϵ expansion. In the static ($\Omega = 0$) and long wavelength limit ($q \rightarrow 0$), the boson propagator in the large N_f approximation has the following form for the momentum dependence:

$$D(i\omega = 0, \mathbf{q} \rightarrow 0)^{-1} \sim q_\perp + |q_z|. \quad (\text{S70})$$

Let us consider the ϵ expansion case. In the ϵ expansion, near the interacting fixed point,

$$\alpha^* \gamma^* = \frac{\epsilon}{N_f} \left(1 - \frac{c_{N_f}}{N_f}\right) \approx \frac{\epsilon}{N_f}, \quad (\text{S71})$$

$$\frac{\alpha^*}{\gamma^*} = \frac{\epsilon}{N_f} \frac{1}{1 - c_{N_f}/N_f} \approx \frac{\epsilon}{N_f} \left(1 + \frac{c_{N_f}}{N_f}\right) \approx \frac{\epsilon}{N_f}, \quad (\text{S72})$$

where we only keep up to N_f^{-1} order because we consider the large N_f limit. Using these results,

$$\begin{aligned}
D(i\omega = 0, \mathbf{q} \rightarrow 0)^{-1} &= a q_\perp^2 + \frac{1}{a} q_z^2 - \Pi(i\omega, \mathbf{q}) \\
&= a \left(1 + N_f \frac{\alpha^*}{\gamma^*} \ell\right) q_\perp^2 + \frac{1}{a} (1 + N_f \alpha^* \gamma^* \ell) q_z^2 \\
&\approx a (1 + \epsilon \ell) q_\perp^2 + \frac{1}{a} (1 + \epsilon \ell) q_z^2 \\
&\sim e^{\epsilon \ell} q_\perp^2 + e^{\epsilon \ell} q_z^2 \\
&\approx q_\perp^{2-\epsilon/z_\perp} + |q_z|^{2-\epsilon}. \quad (\text{S73})
\end{aligned}$$

Here, in the fourth line, we absorbed the momentum dependence of a into q_\perp and q_z . For a sufficiently large N_f , $z_\perp \approx 1$, thus for $\epsilon = 1$ with $d = 3$, $D(0, \mathbf{q})^{-1} \sim q_\perp + |q_z|$. Therefore, the result of the ϵ expansion is consistent with the large N_f calculation.

IV. PHYSICAL OBSERVABLES IN THE NON-INTERACTING LIMIT

In this section, we will calculate the physical observables such as the specific heat, compressibility, diamagnetic susceptibility, and optical conductivity at the TQPT between DWSM and insulating phases in the non-interacting limit. For simplicity, we assume $t_x = t_y = t_\perp$, the rotational symmetry along the k_z -axis.

A. Density of states

Through the analytic continuation $i\omega \rightarrow \omega + i\delta$ in $G_0(i\omega, \mathbf{k})$, the retarded Green's function G_0^{ret} is obtained as

$$G_0^{\text{ret}}(\omega + i\delta, \mathbf{k}) = \frac{1}{-(\omega + i\delta) + \mathcal{H}_0(\mathbf{k})}, \quad (\text{S74})$$

and the imaginary part of G_0^{ret} and the spectral function are

$$\text{Im}[G_0^{\text{ret}}(\omega, \mathbf{k})] = \frac{\pi \text{sgn}(\omega)}{2E_k} (\omega + \mathcal{H}_0(\mathbf{k})) (\delta(\omega - E_k) + \delta(\omega + E_k)), \quad (\text{S75})$$

$$\begin{aligned} S_F(\omega) &= -\frac{1}{\pi} \text{Tr}[G_0^{\text{ret}}(\omega, \mathbf{k})] \\ &= \delta(\omega + E_k) + \delta(\omega - E_k). \end{aligned} \quad (\text{S76})$$

The density of states is given by

$$\begin{aligned} \rho(\omega) &= \int \frac{d^3k}{(2\pi)^3} S_F(\omega, \mathbf{k}) \\ &= \frac{|\omega|}{\pi^2} \int_0^\infty dk_\perp \int_0^\infty dk_z k_\perp \delta(\omega^2 - (t_\perp^2 k_\perp^4 + t_z^2 k_z^4)) \\ &= \frac{\Gamma(5/4)}{4\pi^{3/2}\Gamma(3/4)} \frac{|\omega|^{1/2}}{t_\perp t_z^{1/2}}, \end{aligned} \quad (\text{S77})$$

where $\Gamma(x)$ is the gamma function and we use the identity,

$$\int_0^1 dR \frac{R}{(1-R^4)^{3/4}} = \frac{\sqrt{\pi}\Gamma(5/4)}{\Gamma(3/4)}. \quad (\text{S78})$$

B. Free energy

In this section, we will calculate the free energy at the TQPT in the non-interacting limit from which the specific heat and the compressibility are derived. The finite-temperature propagator of fermion is

$$G_0(i\omega_n, \mathbf{k})^{-1} = (-i\omega_n - \mu) + \mathcal{H}_0(\mathbf{k}), \quad (\text{S79})$$

where we introduce the chemical potential μ for deriving the compressibility. The partition function and its logarithmic form are given by

$$\begin{aligned} \mathcal{Z} &= \text{Det}[\beta G_0^{-1}] \\ &= \prod_{i\omega_n} \prod_{\mathbf{k}} [\beta^2 ((\omega_n - i\mu)^2 + E(\mathbf{k})^2)], \end{aligned} \quad (\text{S80})$$

$$\begin{aligned} \ln \mathcal{Z} &= V \int \frac{d^3k}{(2\pi)^3} T \sum_{i\omega_n} \ln [\beta^2 ((\omega_n - i\mu)^2 + E(\mathbf{k})^2)] \\ &= \frac{V}{2} \int \frac{d^3k}{(2\pi)^3} T \sum_{i\omega_n} [\ln \{\beta^2 (\omega_n^2 + (E(\mathbf{k}) - \mu)^2)\} + \ln \{\beta^2 (\omega_n^2 + (E(\mathbf{k}) + \mu)^2)\}], \end{aligned} \quad (\text{S81})$$

where $\beta = T^{-1}$ and we use the relation

$$[(\omega_n - i\mu)^2 + E(\mathbf{k})^2] [(\omega_n + i\mu)^2 + E(\mathbf{k})^2] = [\omega_n^2 + (E(\mathbf{k}) - \mu)^2] [\omega_n^2 + (E(\mathbf{k}) + \mu)^2]. \quad (\text{S82})$$

By using

$$\sum_{i\omega_n} \ln [\beta^2(\omega_n^2 + E(\mathbf{k})^2)] = E(\mathbf{k})/T + 2 \ln(1 + e^{-E(\mathbf{k})/T}) + \text{const.}, \quad (\text{S83})$$

we obtain the free energy density as

$$\begin{aligned} \mathcal{F} &= -\frac{T}{V} \ln \mathcal{Z} \\ &= -T \int \frac{d^3k}{(2\pi)^3} \left[E(\mathbf{k})/T + \ln(1 + e^{-(E(\mathbf{k})-\mu)/T}) + \ln(1 + e^{-(E(\mathbf{k})+\mu)/T}) + \text{const.} \right]. \end{aligned} \quad (\text{S84})$$

Subtracting $T = 0$ contribution, $\delta\mathcal{F}(T) := \mathcal{F}(T) - \mathcal{F}(0)$ is given by

$$\begin{aligned} \delta\mathcal{F}(T, \mu) &= -T \int \frac{d^3k}{(2\pi)^3} \left[\ln(1 + e^{-(E(\mathbf{k})-\mu)/T}) + \ln(1 + e^{-(E(\mathbf{k})+\mu)/T}) \right] \\ &= \frac{\Gamma(5/4)}{8\pi\Gamma(3/4)} \frac{T^{5/2}}{t_\perp t_z^{1/2}} \left[\text{Li}_{\frac{5}{2}}(-e^{\mu/T}) + \text{Li}_{\frac{5}{2}}(-e^{-\mu/T}) \right], \end{aligned} \quad (\text{S85})$$

where $\text{Li}_n(x)$ is the polylogarithm function.

1. Specific heat

For $\mu = 0$, using $\text{Li}_{\frac{5}{2}}(-1) = -\frac{(4-\sqrt{2})}{4}\zeta(5/2)$ with the zeta function $\zeta(x)$, we get the free energy $\delta\mathcal{F}(T, 0)$ as

$$\delta\mathcal{F}(T, 0) = -\frac{(4-\sqrt{2})\Gamma(5/4)\zeta(5/2)}{16\pi\Gamma(3/4)} \frac{T^{5/2}}{t_\perp t_z^{1/2}}. \quad (\text{S86})$$

The specific heat at $\mu = 0$ is then given by

$$\begin{aligned} C_V &= -T \frac{\partial^2 \delta\mathcal{F}(T, 0)}{\partial T^2} \\ &= \frac{15(4-\sqrt{2})\Gamma(5/4)\zeta(5/2)}{64\pi\Gamma(3/4)} \frac{T^{3/2}}{t_\perp t_z^{1/2}}. \end{aligned} \quad (\text{S87})$$

2. Compressibility

The compressibility is given by

$$\begin{aligned} \kappa &= -\frac{\partial^2 \delta\mathcal{F}(T, \mu)}{\partial \mu^2} \\ &= -\frac{\Gamma(5/4)}{8\pi\Gamma(3/4)} \frac{T^{1/2}}{t_\perp t_z^{1/2}} \left[\text{Li}_{\frac{1}{2}}(-e^{\mu/T}) + \text{Li}_{\frac{1}{2}}(-e^{-\mu/T}) \right]. \end{aligned} \quad (\text{S88})$$

At $\mu = 0$, we have

$$\kappa = -\frac{(\sqrt{2}-1)\Gamma(5/4)\zeta(1/2)}{4\pi\Gamma(3/4)} \frac{T^{1/2}}{t_\perp t_z^{1/2}}, \quad (\text{S89})$$

where $\text{Li}_{1/2}(-1) = (\sqrt{2}-1)\zeta(1/2)$ is used. Note that $\zeta(1/2) < 0$, hence, $\kappa > 0$.

(S90)

C. Diamagnetic susceptibility

Using the Fukuyama formula [1], the diamagnetic susceptibility is given by

$$\chi_{D,x} = e_0^2 T \sum_{i\omega_n} \int \frac{d^3 k}{(2\pi)^3} \text{Tr}[J_j G(i\omega_n, \mathbf{k}) J_k G(i\omega_n, \mathbf{k}) J_j G(i\omega_n, \mathbf{k}) J_k G(i\omega_n, \mathbf{k})], \quad (\text{S91})$$

where $J_i \equiv \frac{\partial \mathcal{H}_0}{\partial k_i}$ is the current operator,

$$J_x = 2t_\perp k_x \sigma_x + 2t_\perp k_y \sigma_y, \quad (\text{S92})$$

$$J_y = -2t_\perp k_y \sigma_x + 2t_\perp k_x \sigma_y, \quad (\text{S93})$$

$$J_z = 2t_z k_z \sigma_z. \quad (\text{S94})$$

Note that because of the C_4 symmetry of the Hamiltonian, $\chi_{D,x} = \chi_{D,y} = \chi_{D,\perp}$. Subtracting the zero temperature contribution to obtain a finite result, we have

$$\begin{aligned} \chi_{D,\perp} &= e_0^2 T \sum_{i\omega_n} \int \frac{d^3 k}{(2\pi)^3} \text{Tr}[J_y G(i\omega_n, \mathbf{k}) J_z G(i\omega_n, \mathbf{k}) J_y G(i\omega_n, \mathbf{k}) J_z G(i\omega_n, \mathbf{k})] \\ &\quad - e_0^2 \int \frac{d\omega d^3 k}{(2\pi)^4} \text{Tr}[J_y G(i\omega, \mathbf{k}) J_z G(i\omega, \mathbf{k}) J_y G(i\omega, \mathbf{k}) J_z G(i\omega, \mathbf{k})], \\ &= e_0^2 t_\perp^2 t_z^2 \int \frac{d^3 k}{(2\pi)^3} [-32(k_x^2 + k_y^2)k_z^2 M_2 + 128t_\perp^2 t_z^2 (k_x^2 + k_y^2)^3 k_z^6 M_4] \\ &= e_0^2 t_z^{1/2} T^{1/2} c_{\chi,\perp}, \end{aligned} \quad (\text{S95})$$

where $c_{\chi,\perp} = 0.054$. Here, we use

$$\int_0^{\pi/2} \cos \theta_R \sin^{1/2} \theta_R d\theta_R = \frac{2}{3}, \quad (\text{S96})$$

$$\int_0^{\pi/2} \cos^3 \theta_R \sin^{5/2} \theta_R d\theta_R = \frac{8}{77}, \quad (\text{S97})$$

and the following Matsubara frequency summations (where the zero-temperature contribution has been subtracted)

$$\begin{aligned} M_1(\xi/T) &= T \sum_{i\omega_n} \frac{1}{(\omega_n^2 + \xi^2)} - \int_{-\infty}^{\infty} \frac{d\omega}{2\pi} \frac{1}{(\omega^2 + \xi^2)} \\ &= \frac{1}{2\xi} \left[\tanh\left(\frac{\xi}{2T}\right) - 1 \right], \end{aligned} \quad (\text{S98})$$

$$\begin{aligned} M_2(\xi/T) &= T \sum_{i\omega_n} \frac{1}{(\omega_n^2 + \xi^2)^2} - \int_{-\infty}^{\infty} \frac{d\omega}{2\pi} \frac{1}{(\omega^2 + \xi^2)^2} \\ &= \frac{1}{4\xi^3} \left[\tanh\left(\frac{\xi}{2T}\right) - 1 \right] - \frac{1}{8\xi^2 T} \frac{1}{\cosh^2\left(\frac{\xi}{2T}\right)}, \end{aligned} \quad (\text{S99})$$

$$\begin{aligned} M_3(\xi/T) &= T \sum_{i\omega_n} \frac{1}{(\omega_n^2 + \xi^2)^3} - \int_{-\infty}^{\infty} \frac{d\omega}{2\pi} \frac{1}{(\omega^2 + \xi^2)^3} \\ &= \frac{3}{16\xi^5} \left[\tanh\left(\frac{\xi}{2T}\right) - 1 \right] - \frac{3}{32\xi^4 T} \frac{1}{\cosh^2\left(\frac{\xi}{2T}\right)} - \frac{1}{32\xi^3 T^2} \frac{\tanh\left(\frac{\xi}{2T}\right)}{\cosh^2\left(\frac{\xi}{2T}\right)}, \end{aligned} \quad (\text{S100})$$

$$\begin{aligned} M_4(\xi/T) &= T \sum_{i\omega_n} \frac{1}{(\omega_n^2 + \xi^2)^4} - \int_{-\infty}^{\infty} \frac{d\omega}{2\pi} \frac{1}{(\omega^2 + \xi^2)^4} \\ &= \frac{5}{32\xi^7} \left[\tanh\left(\frac{\xi}{2T}\right) - 1 \right] - \frac{5}{64\xi^6 T} \frac{1}{\cosh^2\left(\frac{\xi}{2T}\right)} - \frac{1}{32\xi^5 T^2} \frac{\tanh\left(\frac{\xi}{2T}\right)}{\cosh^2\left(\frac{\xi}{2T}\right)} \end{aligned}$$

$$+ \frac{1}{384\xi^4 T^3} \frac{1}{\cosh^4\left(\frac{\xi}{2T}\right)} \left[2 - \cosh\left(\frac{\xi}{T}\right) \right]. \quad (\text{S101})$$

Similarly, $\chi_{D,z}$ is given by

$$\begin{aligned} \chi_{D,z} &= e_0^2 T \sum_{i\omega_n} \int \frac{d^3 k}{(2\pi)^3} \text{Tr}[J_x G(i\omega_n, \mathbf{k}) J_z G(i\omega_n, \mathbf{k}) J_x G(i\omega_n, \mathbf{k}) J_z G(i\omega_n, \mathbf{k})] \\ &\quad - e_0^2 \int \frac{d\omega d^3 k}{(2\pi)^4} \text{Tr}[J_x G(i\omega, \mathbf{k}) J_z G(i\omega, \mathbf{k}) J_x G(i\omega, \mathbf{k}) J_z G(i\omega, \mathbf{k})] \\ &= e_0^2 t_\perp^4 \int \frac{d^3 k}{(2\pi)^3} [-32(k_x^2 + k_y^2)^2 M_2 + 256t_\perp^4 (k_x^2 + k_y^2)^4 k_x^2 k_y^2 M_4], \\ &= \frac{e_0^2 t_\perp}{t_z^{1/2}} T^{1/2} c_{\chi,z}, \end{aligned} \quad (\text{S102})$$

where $c_{\chi,z} = 0.107$. Here, we used

$$\int_0^{\pi/2} d\theta \frac{\cos^2 \theta}{\sqrt{\sin \theta}} = \frac{4\pi^{1/2}\Gamma(5/4)}{3\Gamma(3/4)}, \quad (\text{S103})$$

$$\int_0^{\pi/2} d\theta \frac{\cos^6 \theta}{\sqrt{\sin \theta}} = \frac{80\pi^{1/2}\Gamma(5/4)}{77\Gamma(3/4)}. \quad (\text{S104})$$

In summary,

$$\chi_{D,\perp} = c_{\chi,\perp} e_0^2 t_z^{1/2} T^{1/2}, \quad \chi_{D,z} = c_{\chi,z} \frac{e_0^2 t_\perp}{t_z^{1/2}} T^{1/2}. \quad (\text{S105})$$

D. Optical conductivity

The optical conductivity is given by

$$\sigma_{ij}(\Omega, T) = e_0^2 \int_{-\infty}^{\infty} \frac{d\omega}{\pi} \frac{n_F(\omega) - n_F(\omega + \Omega)}{\Omega} \int \frac{d^3 k}{(2\pi)^3} \text{Tr} [J_i \text{Im}[G_0^{\text{ret}}(\omega, \mathbf{k})] J_j \text{Im}[G_0(\omega + \Omega, \mathbf{k})]], \quad (\text{S106})$$

where $n_F(x) = \frac{1}{1+e^{x/T}}$. Because of the C_4 symmetry of the Hamiltonian, $\sigma_{xx} = \sigma_{yy}$. Hence, we only need to consider σ_{xx} and σ_{zz} .

$$\begin{aligned} \sigma_{xx}(\Omega, T) &= e_0^2 \int_{-\infty}^{\infty} \frac{d\omega}{\pi} \frac{n_F(\omega) - n_F(\omega + \Omega)}{\Omega} \int \frac{d^3 k}{(2\pi)^3} \text{Tr} [J_x \text{Im}[G_0^{\text{ret}}(\omega, \mathbf{k})] J_x \text{Im}[G_0^{\text{ret}}(\omega + \Omega, \mathbf{k})]] \\ &= \frac{e_0^2 T^{3/2}}{5t_z^{1/2}} \delta(\Omega) \int_0^\infty dR \frac{R^{3/2}}{\cosh^2\left(\frac{R}{2}\right)} + \frac{3}{20\sqrt{2}\pi} \frac{e_0^2}{t_z^{1/2}} |\Omega|^{1/2} \tanh\left(\frac{|\Omega|}{4T}\right), \end{aligned} \quad (\text{S107})$$

$$\begin{aligned} \sigma_{zz}(\Omega, T) &= e_0^2 \int_{-\infty}^{\infty} \frac{d\omega}{\pi} \frac{n_F(\omega) - n_F(\omega + \Omega)}{\Omega} \int \frac{d^3 k}{(2\pi)^3} \text{Tr} [J_z \text{Im}[G_0^{\text{ret}}(\omega, \mathbf{k})] J_z \text{Im}[G_0(\omega + \Omega, \mathbf{k})]] \\ &= \frac{e_0^2 T^{3/2}}{t_\perp t_z^{-1/2}} \frac{3\Gamma(-1/4)^2}{160\sqrt{2}\pi^{5/2}} \delta(\Omega) \int_0^\infty dR \frac{R^{3/2}}{\cosh^2\left(\frac{R}{2}\right)} + \frac{\sqrt{\pi}\Gamma(3/4)}{40\sqrt{2}\Gamma(5/4)} \frac{e_0^2}{t_\perp t_z^{-1/2}} |\Omega|^{1/2} \tanh\left(\frac{|\Omega|}{4T}\right). \end{aligned} \quad (\text{S108})$$

Here, we used the following identities,

$$\int_0^\infty dR \frac{R^{3/2}}{\cosh^2\left(\frac{R}{2}\right)} = 4.06856, \quad (\text{S109})$$

$$\int_0^{\pi/2} \frac{\cos^{7/2} \theta}{\sqrt{\cos \theta \sin \theta}} d\theta = \frac{8}{5}, \quad (\text{S110})$$

$$\int_0^{\pi/2} \sin^{5/2} \theta d\theta = \frac{3\Gamma(-1/4)^2}{40\sqrt{2}\pi}, \quad (\text{S111})$$

$$\int_0^1 dR \frac{R^3(R^4 - 2)}{(1 - R^4)^{3/4}} = -\frac{6}{5}, \quad (\text{S112})$$

$$\int_0^1 dR \frac{R^5}{\sqrt{1 - R^4}} = \frac{\sqrt{\pi}\Gamma(3/4)}{10\Gamma(5/4)}, \quad (\text{S113})$$

$$\lim_{\Omega \rightarrow 0} \frac{n_F(A) - n_F(A \pm \Omega)}{\Omega} = \pm \frac{1}{4T} \frac{1}{\cosh^2(A/2T)}. \quad (\text{S114})$$

For $T = 0$,

$$\sigma_{xx}(\Omega) = \frac{3}{20\sqrt{2}\pi} \frac{e_0^2}{t_z^{1/2}} |\Omega|^{1/2}, \quad \sigma_{zz}(\Omega) = \frac{\sqrt{\pi}\Gamma(3/4)}{40\sqrt{2}\Gamma(5/4)} \frac{e_0^2}{t_\perp t_z^{-1/2}} |\Omega|^{1/2}. \quad (\text{S115})$$

V. EFFECT OF EXTRA RELEVANT PERTURBATIONS

In the presence of extra perturbations such as doping and disorder, a new parameter is introduced to characterize the extra perturbation in addition to the intrinsic length scale, correlation length ξ set by temperature. For example, for doping, the Fermi wave vector k_F is well defined. With the two parameters, the two regimes naturally appear. For a large doping $k_F \xi \gg 1$, our fixed point cannot be a good starting point, and it would be better to start from the Fermi liquid. On the other hand, $k_F \xi \ll 1$, our description is certainly a good starting point and one can investigate the doping effect as a perturbation even though a little more additional cautions are necessary as in one of the standard critical phenomena.

VI. SANITY CHECK OF THE POWER-LAW CORRECTION

In the main text, we included all the renormalization effects in the system parameters. Here, for a sanity check, equivalently we will include all the renormalization effects in the coordinates and obtain the associated anomalous dimensions.

Recall that the RG equations for t_\perp and t_z are given by

$$\frac{1}{t_\perp} \frac{dt_\perp}{d\ell} = z - 2z_\perp + \alpha F_\perp(\gamma), \quad (\text{S116})$$

$$\frac{1}{t_z} \frac{dt_z}{d\ell} = z - 2 + \alpha F_z(\gamma). \quad (\text{S117})$$

Imposing t_\perp and t_z as constants, then we have

$$z = 2 - \alpha F_z(\gamma), \quad (\text{S118})$$

$$z_\perp = 1 + \frac{\alpha}{2} [F_\perp(\gamma) - F_z(\gamma)]. \quad (\text{S119})$$

At the fixed point $(\alpha, \gamma) = (\alpha^*, \gamma^*)$,

$$z^* = 2 - \alpha^* F_z(\gamma^*), \quad (\text{S120})$$

$$z_\perp^* = 1 + \frac{\alpha^*}{2} [F_\perp(\gamma^*) - F_z(\gamma^*)]. \quad (\text{S121})$$

Now, let us find the power-law corrections of the physical observables by using scaling hypothesis with the renormalized quantity \mathcal{O}_R and the scaling dimension $d_{\mathcal{O}}$ for an observable \mathcal{O} . For the density of states, we have

$$\rho = b^{z - (2z_\perp + 1)} \rho_R, \quad (\text{S122})$$

whereas for the free energy,

$$\mathcal{F} = b^{-(z + 2z_\perp + 1)} \mathcal{F}_R. \quad (\text{S123})$$

From Eq. (S123), we obtain the specific heat and the compressibility, respectively, as

$$C_V = -T \frac{\partial^2 \mathcal{F}}{\partial T^2} = b^{-(2z_\perp + 1)} C_{V,R}, \quad (\text{S124})$$

$$\kappa = -\frac{\partial^2 \mathcal{F}}{\partial \mu^2} = b^{z-(2z_\perp+1)} \kappa_R. \quad (\text{S125})$$

To determine the scaling relation of the optical conductivities and the diamagnetic susceptibilities, we use the minimal coupling $-i\partial_i \rightarrow -i\partial_i + e_0 A_i(\tau, \mathbf{x})$, where $A_i(\tau, \mathbf{x})$ is a gauge-field. Since e_0 receives no renormalization at all, the scaling dimension of A_i is the same as that of ∂_i . The optical conductivities and the diamagnetic susceptibilities can be obtained from the current-current response function $K_{ij}(i\omega, \mathbf{q}) = \frac{1}{(2\pi)^{d+1} \delta(\omega+\Omega) \delta^d(\mathbf{q}+\mathbf{p})} \langle \mathcal{J}_i(i\omega, \mathbf{q}) \mathcal{J}_j(i\Omega, \mathbf{p}) \rangle$ with $\mathcal{J}_i(i\omega, \mathbf{q}) = e_0 \int_{\mathbf{k}} \psi^\dagger(i\omega, \mathbf{k} + \mathbf{q}) \frac{\partial \mathcal{H}_0(\mathbf{k})}{\partial k_i} \psi(i\omega, \mathbf{k})$ by the following relations [1, 2]:

$$\sigma_{ij}(\omega) = \frac{1}{2\omega} \text{Im} K_{ij}^{\text{ret}}(\omega, \mathbf{q} = \mathbf{0}), \quad (\text{S126})$$

$$\chi_{D,i}(\omega) = -\lim_{\mathbf{q} \rightarrow \mathbf{0}} \frac{\epsilon_{ijk}}{2q_j q_k} K_{jk}(0, \mathbf{q}). \quad (\text{S127})$$

Here, the repeated indices are not summed. Because $\langle \mathcal{J}_i(i\omega, \mathbf{q}) \mathcal{J}_j(i\Omega, \mathbf{p}) \rangle$ is obtained by differentiating the logarithm of the partition function $Z[\mathbf{A}]$ with respect to $A_i(i\omega, \mathbf{q})$ and $A_j(i\Omega, \mathbf{p})$, the scaling dimension of $K_{ij}(i\omega, \mathbf{q})$, namely $[K_{ij}]$, is given by

$$\begin{aligned} [K_{ij}] &= \left[\frac{\delta}{\delta A_i(i\omega, \mathbf{q})} \right] + \left[\frac{\delta}{\delta A_j(i\Omega, \mathbf{p})} \right] - [d\tau] - [d^d \mathbf{x}] \\ &= -[\partial_i] - [\partial_j] + (z + 2z_\perp + d - 2). \end{aligned} \quad (\text{S128})$$

Equipped with this scaling relation of K_{ij} , we can derive the following relations:

$$\sigma_{\perp\perp} = b^{d-2} \sigma_{\perp\perp, R}, \quad (\text{S129})$$

$$\sigma_{zz} = b^{2z_\perp - d + 2} \sigma_{zz, R}, \quad (\text{S130})$$

$$\chi_{D, \perp} = b^{-z + d - 2} \chi_{D, \perp, R}, \quad (\text{S131})$$

$$\chi_{D, z} = b^{-z + 2z_\perp - d + 2} \chi_{D, z, R}. \quad (\text{S132})$$

The RG equation of the temperature and frequency is

$$\frac{d\mathcal{O}}{d \ln b} = z\mathcal{O}, \quad (\text{S133})$$

where $\mathcal{O} = T, \Omega$. Let $z = z^*$ and $z_\perp = z_\perp^*$. Solving this, we obtain $\mathcal{O}(b) = b^{z^*} \mathcal{O}$. Let b^* be the cutoff value, so that $\mathcal{O}(b^*) = (b^*)^{z^*} \mathcal{O} = \Lambda$, then $b^* = (\Lambda/\mathcal{O})^{1/z^*} \propto \mathcal{O}^{-1/z^*}$. Using this, we can obtain the power-law corrections of the observables in terms of the temperature and frequency.

For the density of states, we have

$$\rho \propto |\Omega|^{(2z_\perp^* + 1 - z^*)/z^*} \propto |\Omega|^{1/2 + c_\perp + \frac{1}{2}c_z}. \quad (\text{S134})$$

For the specific heat and compressibility,

$$C_V \propto T^{(2z_\perp^* + 1)/z^*} \approx T^{3/2 + c_\perp + \frac{1}{2}c_z}, \quad (\text{S135})$$

$$\kappa \propto T^{(2z_\perp^* + 1 - z^*)/z^*} \approx T^{1/2 + c_\perp + \frac{1}{2}c_z}. \quad (\text{S136})$$

For the diamagnetic susceptibility,

$$\chi_{D, \perp} \propto T^{(z^* - 1)/z^*} \approx T^{1/2 - \frac{1}{2}c_z}, \quad (\text{S137})$$

$$\chi_{D, z} \propto T^{(z^* - 2z_\perp^* + 1)/z^*} \approx T^{1/2 - c_\perp + \frac{1}{2}c_z}. \quad (\text{S138})$$

For the optical conductivity,

$$\sigma_{xx} \propto \Omega^{1/z^*} \approx \Omega^{1/2 + c_z}, \quad (\text{S139})$$

$$\sigma_{zz} \propto \Omega^{(2z_\perp^* - 1)/z^*} \approx \Omega^{1/2 + c_\perp - \frac{1}{2}c_z}. \quad (\text{S140})$$

Here, $c_\perp \approx 0.402/N_f$ and $c_z \approx 0.044/N_f$ in the large N_f approximation. Thus, we obtain the same results as in the main text. If the symmetry-allowed parabolic term is included, we have $c_\perp \approx 0.145/N_f$ and $c_z \approx 0.050/N_f$.

For the candidate materials of DWSM, HgCr_2Se_4 and SrSi_2 , HgCr_2Se_4 has one pair ($N_f = 1$) of double-Weyl points, whereas SrSi_2 has six pairs ($N_f = 6$) of double-Weyl points. In particular, for SrSi_2 , it has cubic symmetry, therefore, to see the anisotropic behaviors, we need to maintain only one C_4 symmetry. For example, if we apply a uniaxial pressure along \hat{z} , then the C_4 symmetry along \hat{x} and \hat{y} is broken, so we only have two pairs of double-Weyl points on the \hat{z} axis [3]. Therefore, under this situation, the effective number of pairs of double-Weyl points of SrSi_2 is two ($N_f = 2$). Then, for $\eta_2 \equiv c_z/2$ and $\eta_3 \equiv c_\perp - c_z/2$ we find that $\eta_2 - \eta_3$ values for HgCr_2Se_4 and SrSi_2 are -0.198 and -0.132 , respectively. We expect that the anisotropic scaling will be manifested at low temperatures or low frequencies.

VII. STABILITY OF THE ANISOTROPIC NFL FIXED POINT UNDER SHORT-RANGE INTERACTIONS

In this section, we study the effect of short-range interactions which was reported to destroy the non-Fermi liquid phase in the pyrochlore iridates $A_2\text{Ir}_2\text{O}_7$ [4, 5] and show that the non-Fermi liquid phase of DWSM at the TQPT remains stable in a realizable range of N_f in $d = 3$.

A. Possible type of short-range interactions

Here, we investigate how short-range interactions affect the non-Fermi liquid we have found. We first note that

$$(\psi^\dagger \sigma_0 \psi)^2 = -(\psi^\dagger \sigma_i \psi)^2 = \frac{1}{2} (\psi^\dagger \sigma_y \psi^*) (\psi^\top \sigma_y \psi) \quad (\text{S141})$$

for $i = x, y, z$. Using this identity, we can study the effects of all possible short-range interactions in the particle-particle and particle-hole channels by adding just the following interaction to the action in Eq. (S19):

$$S_u = \frac{u}{2} \int d\tau d^d x (\psi^\dagger \sigma_0 \psi)_{(\tau, x)}^2. \quad (\text{S142})$$

In contrast to Ref. [4, 5] where the 4 by 4 gamma matrices are used and the vector-type short-range interactions appear, only the scalar-type interaction is needed in the present case.

B. One-loop corrections

To obtain the corrections generated by the short-range interaction and the combination of the short-range and Coulomb interactions up to one-loop order, we evaluate the Feynman diagrams in Fig. S3. Among the diagrams in Fig. S3, only the diagrams Figs. 3(b), 3(g), 3(h), and 3(k) give us the following non-zero corrections to the short-range interaction,

$$\begin{aligned} \delta u^{(b)} dl &= -u^2 \int_{\partial\Lambda} \frac{d\Omega d^d q}{(2\pi)^{d+1}} \eta_{\mu\nu} \frac{\text{Tr}[\sigma_0 G(i\Omega, \mathbf{q}) \sigma_0 \sigma_\mu]}{\text{Tr}[\sigma_\mu \sigma_\mu]} \frac{\text{Tr}[\sigma_0 G(i\Omega, \mathbf{q}) \sigma_0 \sigma_\mu]}{\text{Tr}[\sigma_\mu \sigma_\mu]}, \\ \delta u^{(g),(h)} dl &= u (ig)^2 \int_{\partial\Lambda} \frac{d\Omega d^d q}{(2\pi)^{d+1}} \eta_{\mu\nu} \frac{\text{Tr}[\sigma_0 G(i\Omega, \mathbf{q}) \sigma_0 \sigma_\mu]}{\text{Tr}[\sigma_\mu \sigma_\mu]} \frac{\text{Tr}[\sigma_0 G(i\Omega, \mathbf{q}) \sigma_0 \sigma_\mu]}{\text{Tr}[\sigma_\mu \sigma_\mu]} D_0(i\Omega, \mathbf{q}), \\ \delta u^{(k)} dl &= - (ig)^4 \int_{\partial\Lambda} \frac{d\Omega d^d q}{(2\pi)^{d+1}} \eta_{\mu\nu} \frac{\text{Tr}[\sigma_0 G(i\Omega, \mathbf{q}) \sigma_0 \sigma_\mu]}{\text{Tr}[\sigma_\mu \sigma_\mu]} \frac{\text{Tr}[\sigma_0 G(i\Omega, \mathbf{q}) \sigma_0 \sigma_\mu]}{\text{Tr}[\sigma_\mu \sigma_\mu]} D_0(i\Omega, \mathbf{q})^2, \end{aligned}$$

where $\eta_{\mu\nu} \equiv \text{diag}(1, -1, -1, -1)$ and the repeated indices are summed over. Here, by using Eq. (S141), we convert the corrections to ‘vector-type’ short-range interaction such as $(\psi^\dagger \sigma_i \psi)^2$ ($i = x, y, z$) into the corrections to the ‘scalar-type’ short-range interaction such as $(\psi^\dagger \sigma_0 \psi)^2$, which is reflected in $\eta_{\mu\nu}$. As a result, we obtain the following correction δu to u :

$$\begin{aligned} \delta u dl &= \delta u^{(b)} dl + \delta u^{(g)} dl + \delta u^{(h)} dl + \delta u^{(k)} dl \\ &= - \sum_{a,b=u,g} \int_{\partial\Lambda} \frac{d\Omega d^d q}{(2\pi)^{d+1}} \eta_{\mu\nu} \frac{\text{Tr}[\sigma_0 G(i\Omega, \mathbf{q}) \sigma_0 \sigma_\mu]}{\text{Tr}[\sigma_\mu \sigma_\mu]} \frac{\text{Tr}[\sigma_0 G(i\Omega, \mathbf{q}) \sigma_0 \sigma_\mu]}{\text{Tr}[\sigma_\mu \sigma_\mu]} I_a(\mathbf{q}) I_b(\mathbf{q}) \end{aligned}$$

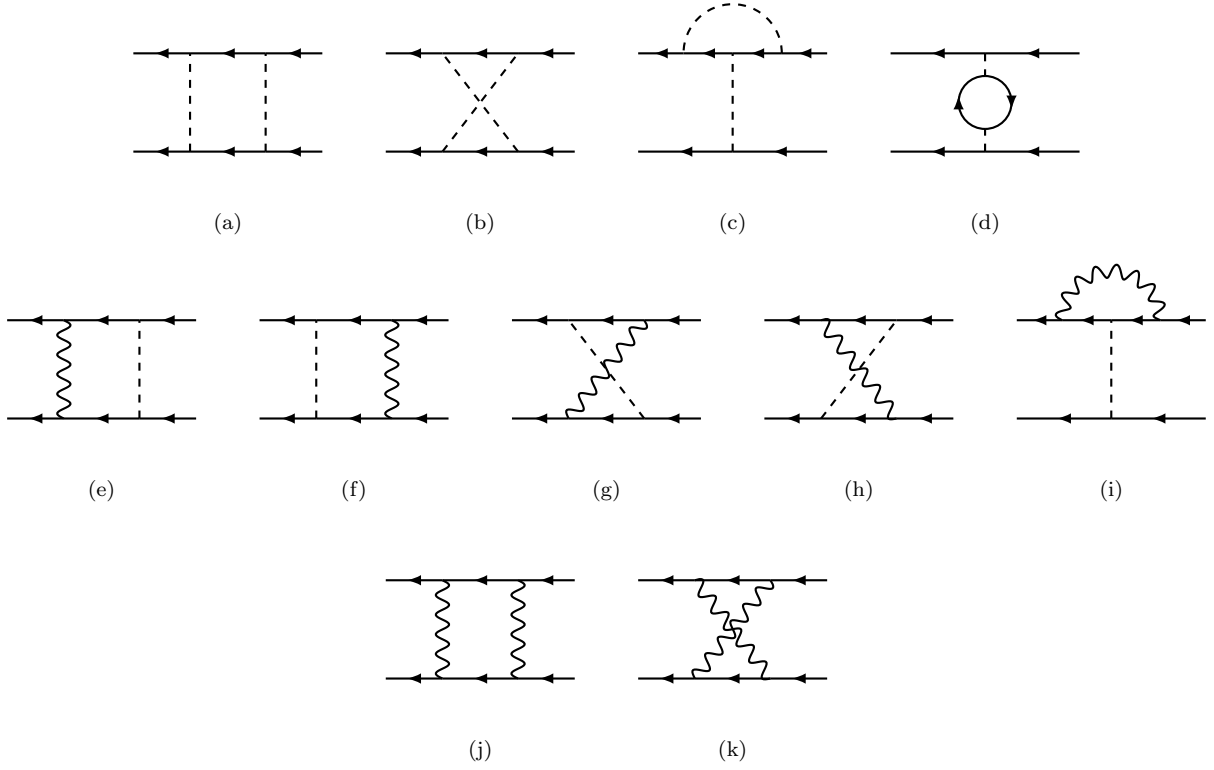


FIG. S3: Feynman diagrams generated by the short-range interaction and long-range Coulomb interaction. The dashed and wavy lines stand for the short-range interaction and long-range Coulomb interaction, respectively. The solid line with an arrowhead stands for the fermion propagator.

$$= \frac{u^2}{4} \int_{\partial\Lambda} \frac{d^d q}{(2\pi)^d} \frac{1}{\varepsilon_{\mathbf{q}}} + \frac{ug^2}{2} \int_{\partial\Lambda} \frac{d^d q}{(2\pi)^d} \frac{1}{aq_{\perp}^2 + \frac{1}{a}q_z^2} \frac{1}{\varepsilon_{\mathbf{q}}} + \frac{g^4}{4} \int_{\partial\Lambda} \frac{d^d q}{(2\pi)^d} \frac{1}{(aq_{\perp}^2 + \frac{1}{a}q_z^2)^2} \frac{1}{\varepsilon_{\mathbf{q}}}, \quad (\text{S143})$$

where $I_u(\mathbf{q}) = u$ and $I_g(\mathbf{q}) = \frac{g^2}{a(k_x^2 + k_y^2) + k_z^2/a}$. Introducing a dimensionless parameter

$$\bar{u} = \frac{S_{d-2}}{4\pi(2\pi)^{d-2} \Lambda^{2-d} |t_{\perp}|} u,$$

the correction δu to the dimensionless \bar{u} is obtained from Eq. (S143),

$$\delta u = \bar{u}^2 H_1(\lambda) + \bar{u} \alpha H_2(\gamma, \lambda) + \alpha^2 H_3(\gamma, \lambda), \quad (\text{S144})$$

with

$$H_1(\gamma, \lambda) = \int_0^{\Lambda\rho} \frac{\rho d\rho}{\sqrt{\rho^4 + (1 + \lambda\rho^2)^2}} \quad (\text{S145})$$

$$= \frac{1}{2\sqrt{1 + \lambda^2}} \log \left[1 + \frac{\sqrt{1 + (\sqrt{1 + \lambda^2} + \lambda)^2}}{\sqrt{1 + \lambda^2} + \lambda} \right],$$

$$H_2(\gamma, \lambda) = 12\gamma \int_0^{\infty} \frac{\rho d\rho}{(1 + 4\gamma^2\rho^2) \sqrt{\rho^4 + (1 + \lambda\rho^2)^2}} \quad (\text{S146})$$

$$= \frac{6\gamma}{\sqrt{1 + (4\gamma^2 - \lambda)^2}} \log \left[\frac{4\gamma^2 \left(4\gamma^2 - \lambda + \sqrt{1 + (4\gamma^2 - \lambda)^2} \right)}{\sqrt{1 + \lambda^2} \sqrt{1 + (4\gamma^2 - \lambda)^2} + \lambda(4\gamma^2 - \lambda) - 1} \right],$$

$$\begin{aligned}
H_3(\gamma, \lambda) &= 36\gamma^2 \int_0^\infty \frac{\rho d\rho}{(1 + 4\gamma^2 \rho^2)^2 \sqrt{\rho^4 + (1 + \lambda \rho^2)^2}} \\
&= 18\gamma^2 \left[\frac{4\gamma^2 - \sqrt{1 + \lambda^2}}{1 + (4\gamma^2 - \lambda)^2} + \frac{(4\gamma^2 - \lambda) \lambda - 1}{(1 + (4\gamma^2 - \lambda)^2)^{3/2}} \log \left[\frac{4\gamma^2 \left\{ \sqrt{1 + (4\gamma^2 - \lambda)^2} - (4\gamma^2 - \lambda) \right\}}{1 - \lambda(4\gamma^2 - \lambda) + \sqrt{(1 + \lambda^2)(1 + (4\gamma^2 - \lambda)^2)}} \right] \right],
\end{aligned} \tag{S147}$$

where $\Lambda_\rho = (1 + \lambda^2)^{-1/4}$ is introduced to regulate the UV divergence in Eq. (S145).

After rescaling the fields and space-time coordinates, we finally obtain the RG flow functions for α , γ , λ and \bar{u} :

$$\frac{1}{\alpha} \frac{d\alpha}{d\ell} = \epsilon - \frac{\alpha}{2} \left[N_f \left\{ \frac{1}{\gamma} \left(\frac{2 + \lambda^2}{2} - \frac{\lambda(5 + 2\lambda^2)}{4\sqrt{1 + \lambda^2}} \right) + \gamma \left(\frac{1 + 2\lambda^2}{\sqrt{1 + \lambda^2}} - 2\lambda \right) \right\} + F_+(\gamma, \lambda) \right], \tag{S148}$$

$$\frac{1}{\gamma} \frac{d\gamma}{d\ell} = \frac{\alpha}{2} \left[N_f \left\{ \frac{1}{\gamma} \left(\frac{2 + \lambda^2}{2} - \frac{\lambda(5 + 2\lambda^2)}{4\sqrt{1 + \lambda^2}} \right) - \gamma \left(\frac{1 + 2\lambda^2}{\sqrt{1 + \lambda^2}} - 2\lambda \right) \right\} + F_-(\gamma, \lambda) \right], \tag{S149}$$

$$\frac{1}{\lambda} \frac{d\lambda}{d\ell} = -\frac{\alpha}{\lambda} \left[4\gamma^2 F_z(\gamma, \lambda) + \lambda F_\perp(\gamma, \lambda) \right], \tag{S150}$$

$$\begin{aligned}
\frac{d\bar{u}}{d\ell} &= (\epsilon - 2 - \alpha F_\perp(\gamma, \lambda)) \bar{u} + \delta \bar{u} \\
&= (\epsilon - 2 - \alpha F_\perp(\gamma, \lambda) + \alpha H_2(\gamma, \lambda)) \bar{u} + H_1(\gamma, \lambda) \bar{u}^2 + H_3(\gamma, \lambda) \alpha^2.
\end{aligned} \tag{S151}$$

Note that no modification arises in Eqs. (S148), (S149), and (S150) even if we include u , because u does not yield self-energy corrections to the fermion ψ and boson ϕ at leading order. For the particle-particle channel, it has the same RG flow equations as the particle-hole channel because they have the same operator form.

C. RG analysis of the short-range interaction

The RG function for \bar{u} in Eq. (S151) includes a term proportional to α^2 . This α^2 correction generates \bar{u} during the RG even if we start with an initial condition $\bar{u}(\ell = 0) = 0$. Consequently, we find no stable fixed point with $N_f = 1$ in $d = 3$. First, let us ignore λ in the RG functions of Eqs. (S148–51). Figure S4 shows the RG flow for $N_f = 4, 4.775$, and 5 in $d = 3$, where stable (unstable) fixed points are denoted by red (blue) points. The green point is the NFL fixed point obtained when the short-range interaction is neglected. As we can see, the lower bound of N_f , N_c , above which a stable fixed point begins to appear is approximately $N_c = 4.775$. This result seems to show that the non-Fermi liquid phase of DWSM at the TQPT is not realizable since $N_f \geq 5$ is not likely to be achievable in a real experiment. However, if we take λ into account, we get a qualitatively different result. Figure S5 shows the RG flow when λ is kept. The estimated lower bound of N_f is about $N_c = 1.883$. Thus, a stable fixed point appear for $N_f = 2$, which is much smaller compared to that obtained when λ is neglected. We expect that DWSM at the TQPT with $N_f = 2$ is accessible in an experiment with SrSi₂ [3]. Although the estimated values of the lower bound of N_f are found to depend on the renormalization scheme, the symmetry-allowed s_\perp -term in DWSM at the TQPT seems to stabilize the non-Fermi liquid phase.

D. Relevance of the short-range interaction in $\mathcal{O}(\epsilon)$ order

In the previous section, we considered the corrections up to one-loop order. However, in the ϵ expansion, we find the anisotropic NFL fixed point up to order of $\mathcal{O}(\epsilon)$. For that reason, near our anisotropic NFL fixed point, α^2 will give us the correction of $\mathcal{O}(\epsilon^2)$. Therefore, if we carefully consider terms of order ϵ , we can ignore α^2 contributions in Eq. (S151) near our anisotropic NFL fixed point. In this situation, the short-range interaction is irrelevant in $d = 3$ for $N_f > N_c = 2.279$ when λ is neglected, whereas N_c become 0.952 if λ is kept. Thus, keeping λ , we find that the non-Fermi liquid phase of DWSM at the TQPT with $N_f = 1$ remains stable in the presence of the short-range interaction up to the accuracy of $\mathcal{O}(\epsilon)$. Note that to properly keep $\mathcal{O}(\epsilon^2)$ contributions, we need to calculate the two-loop order diagrams, which is beyond the scope of the current work.

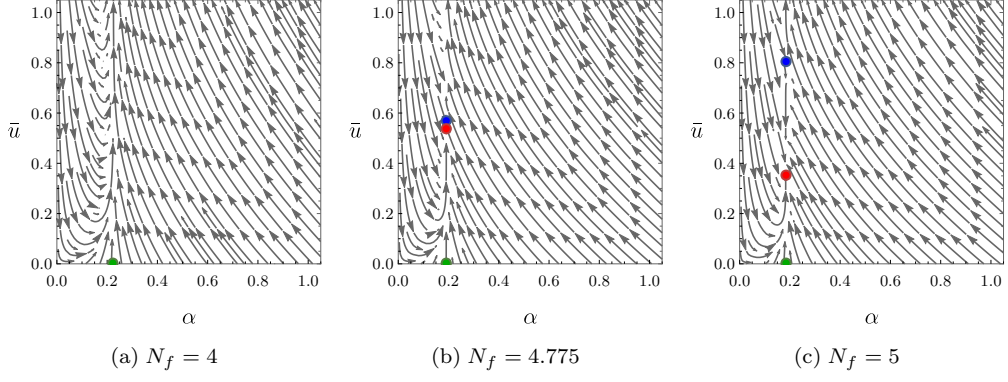


FIG. S4: RG flow diagrams in terms of N_f when s_{\perp} is ignored.

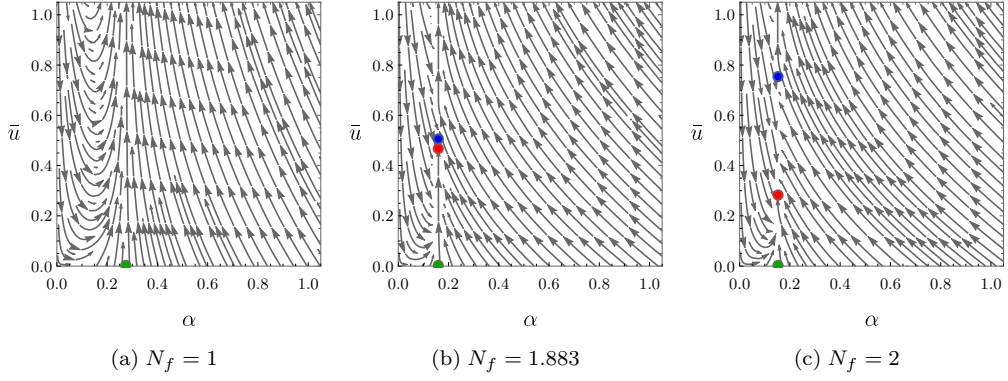


FIG. S5: RG flow diagrams in terms of N_f when s_{\perp} is included.

References

- [1] H. Fukuyama, *Physics Letters A* **32**, 111 (1970).
- [2] D. E. Sheehy and J. Schmalian, *Phys. Rev. Lett.* **99**, 226803 (2007).
- [3] S.-M. Huang, S.-Y. Xu, I. Belopolski, C.-C. Lee, G. Chang, T.-R. Chang, B. Wang, N. Alidoust, G. Bian, M. Neupane, D. Sanchez, H. Zheng, H.-T. Jeng, A. Bansil, T. Neupert, H. Lin, and M. Z. Hasan, *Proceedings of the National Academy of Sciences* **113**, 1180 (2016).
- [4] I. F. Herbut and L. Janssen, *Phys. Rev. Lett.* **113**, 106401 (2014).
- [5] L. Janssen and I. F. Herbut, *Phys. Rev. B* **92**, 045117 (2015).